AN EXPLORATION OF TWO INFINITE FAMILIES OF SNARKS

By

Lander Ver Hoef, B.S.

A Thesis Submitted in Partial Fulfillment of the Requirements

for the Degree of

Master of Science

in

Mathematics

University of Alaska Fairbanks

May 2019

APPROVED:

Dr. Leah Berman, Committee Chair
Dr. Gordon Williams, Committee Member
Dr. Jill Faudree, Committee Member
Dr. Anthony Rickard, Chair
Department of Mathematics
Dr. Leah Berman, Dean
College of Natural Science and Mathematics
Dr. Michael Castellini, *Dean of the Graduate School*

Abstract

In this paper, we generalize a single example of a snark that admits a drawing with even rotational symmetry into two infinite families using a voltage graph construction techniques derived from cyclic Pseudo-Loupekine snarks. We expose an enforced chirality in coloring the underlying 5-pole that generated the known example, and use this fact to show that the infinite families are in fact snarks. We explore the construction of these families in terms of the blowup construction. We show that a graph in either family with rotational symmetry of order m has automorphism group of order $m2^{m+1}$. The oddness of graphs in both families is determined exactly, and shown to increase linearly with the order of rotational symmetry.

Table of Contents

List of Figures

Acknowledgments

Many thanks to my family for giving me unwavering support through the often challenging years of grad school; to my committee for giving encouragement and critique; to the entire UAF mathematics department community for being a delightful group to work and learn with for two years; and to Stella, for endless cat tracks across the keyboard while this thesis was being written.

Chapter 1: Introduction

1.1 General Graph Theory

We begin with a review of certain relevant concepts from graph theory, with most of the terminology coming from the excellent reference by West [18]. Figure 1.1 contains a simple

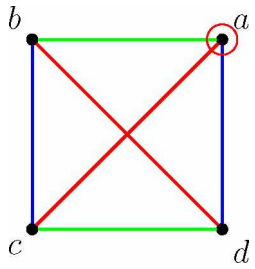

Figure 1.1: The graph K_4, a 3-regular graph on 4 vertices, with a proper 3-edge-coloring, used to illustrate fundamental concepts in graph theory.

example of a *graph*, a collection of points, called *vertices*, and lines joining them, called *edges*. We will call this particular graph K_4. If we look at the highlighted vertex a in K_4, we see that it is incident to 3 edges, so we say that the *degree* of a is 3. Because the degree of all the vertices in K_4 is 3, we say that K_4 is *3-regular*. In Figure 1.1, we have colored the edges of K_4 red, green, and blue. This assignment of colors to edges is called an *edge-coloring*, and because we used 3 colors, it is specifically a *3-edge-coloring*. Moreover, if we examine each of the four vertices of this coloring of K_4, we notice that no vertex is incident with two or more edges of the same color. Thus, this edge-coloring is called *proper*. Throughout the rest of this paper, all edge-colorings are assumed to be proper.

We now define paths and cycles in graphs, which we will use extensively later on. In Figure 1.2, the blue dashed collection of edges P is a *path*. In general, a path is a sequence of edges, with each edge being adjacent to the next, such that the sequence never repeats the same edge or vertex. A path has natural *endpoints*, which are the vertices where the path starts and stops. So, in Figure 1.2, the path P has endpoints a and c. A *cycle* is a

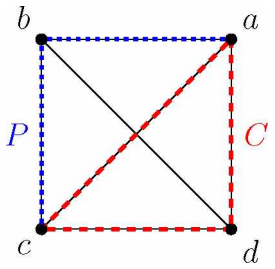

Figure 1.2: The graph K_4, with a highlighted path P and cycle C, used to illustrate fundamental concepts in graph theory.

path where the beginning and ending endpoints are the same vertex. So, the red path C in Figure 1.2 is a cycle through the vertices a, c and d. We define the *length* of a path or cycle to be the number of edges in said path or cycle. Moreover, we will say a cycle is an *even* cycle if it has even length, and *odd* if it has odd length.

We can now also define what it means for a graph to be connected: we say a graph is *connected* if for any pair of vertices u and v, there exists a path from u to v. Clearly, K_4 is connected. Moreover, if we were to remove any single edge from K_4, it would still be connected, so we say that K_4 is *bridgeless*. To link the concepts we presented in Figure 1.1 and Figure 1.2, there is a well-known result in graph theory that a bridgeless 3-regular graph is either 3-edge-colorable or 4-edge-colorable. We are concerned with bridgeless 3-regular graphs that are not 3-edge-colorable, a class which we call *snarks*.

Chapter 2: Introduction to Snarks

2.1 History

For an excellent review of the early history of snarks, see J.J. Watkins' "Snarks" paper [17]. We owe the name snarks to Martin Gardner, who introduced it in a paper in Scientific American in 1976 [5]. However, the study of snarks originated nearly a hundred years before that, when in 1880, P.G. Tait showed that the famous four-color-map theorem was equivalent to that statement that no 3-regular bridgeless non-3-edge-colorable graph was planar (could be drawn without lines crossing). Tait conjectured that every bridgeless 3-regular graph could be 3-edge-colored, a hypothesis that was disproved in 1898 when Julius Petersen discovered the first snark: the Petersen graph, which is shown in Figure 2.1.

As it is an important result, we reprove that the Petersen graph is, in fact, a snark.

Lemma 1. *The Petersen graph is a snark.*

Proof. Suppose to produce a contradiction that the Petersen graph is 3-edge-colorable. Then there exists a proper 3-edge-coloring, and in such an edge-coloring, we must 3-edge-color the outer 5-cycle. When we do so, we must end up with two edges of one color (which we will call green), two edges of another (which we will call red), and one edge of a third (which we will call blue). By the symmetry of the Petersen graph, any arrangement of these colored edges on the outer 5-cycle is in fact equivalent, so we may choose a particular arrangement without loss of generality. In any 3-edge-coloring of a 3-regular graph, once two edges at a vertex have been assigned a color, the color of the third edge is entirely determined, so the colors of the "spokes" between the pentagon and the pentagram are determined by our arrangement of colors on the outer cycle. The coloring so far is shown in Figure 2.1.

At this point, we note that the vertex x has a green edge already incident to it and y is incident with a blue edge. Thus, in any proper 3-edge-coloring, the edge xy must be red. However, z is also incident with a blue edge, so the edge xz must also be red, and the coloring

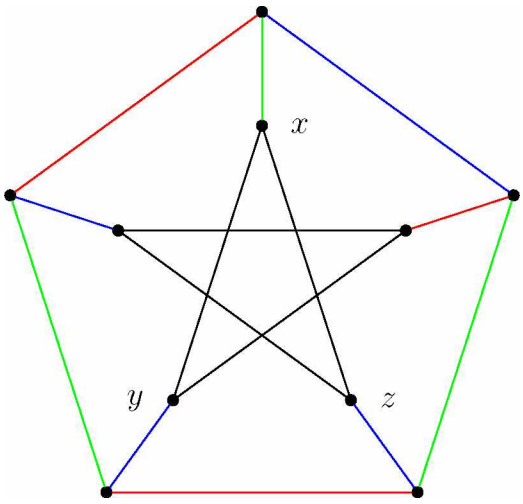

Figure 2.1: An illustration of why the Petersen graph is not 3-edge-colorable.

is not proper. Thus, to achieve a proper edge-coloring, we need a fourth color, contradicting our assumption that the Petersen graph is 3-edge-colorable. □

For nearly fifty years, the Petersen graph was the only known snark. Eventually, three more distinct snarks were found, one each by Danilo Blanuša in 1946, Blanche Descartes (a pseudonym for W.T. Tutte) in 1948 and George Szekeres in 1973. In 1975, Rufus Isaacs revolutionized snark hunting by discovering the first infinite family of snarks (called the *BDS* or *Blanuša-Descartes-Szekeres snarks*), of which the previous three examples were specific cases, and an entirely new family called *flower snarks* [10]. The following year, Isaacs published another paper based on his correspondence with a graduate student, Feodor Loupekine, in which Loupekine outlined the construction of another infinite family of snarks, now known as Loupekine Snarks [11]. We will discuss these further below.

2.2 Motivation

Why study snarks? This class of graphs has mostly proved interesting as a source for potential counterexamples to conjectures. As we discussed above, the first snark was a counterexample to the conjecture that the four-color-map theorem held because all 3-regular graphs were 3-edge-colorable. The hunt continued, however, since disproving the four-color-

map theorem became equivalent to finding a planar snark. Because the four-color-map theorem has since been proved through other methods [1] we now know that no snark is planar.

More recently, the Berge-Fulkerson conjecture, first outlined in [15], conjectures that for every bridgeless cubic graph, there exist 6 perfect matchings with the property that every edge appears in exactly two perfect matchings. A *perfect matching* is a set of edges M such that every vertex in the graph is incident with exactly one edge in M. Six examples of perfect matchings are shown in Figure 2.2.

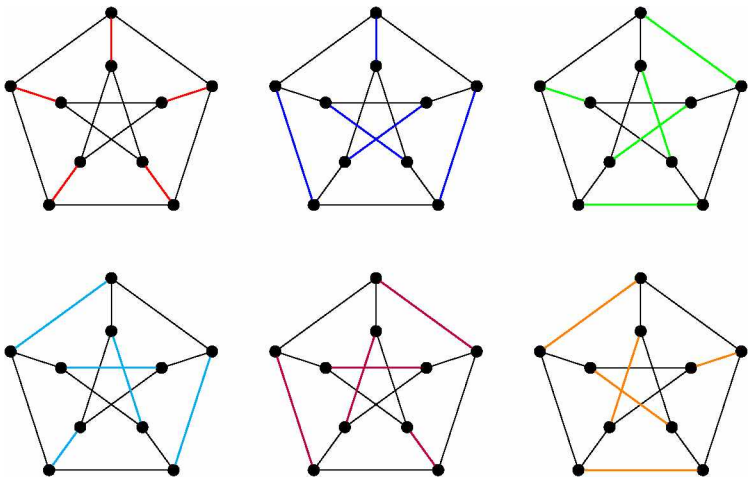

Figure 2.2: Six perfect matchings on the Petersen graph, with each edge appearing in precisely two matchings.

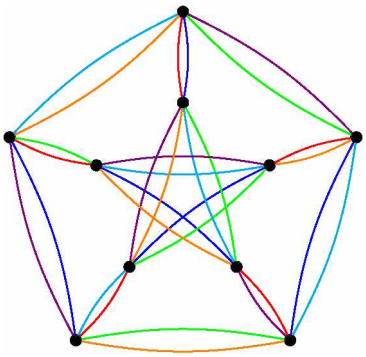

Figure 2.3: The six perfect matchings from Figure 2.2, shown on the Petersen graph with doubled edges, demonstrating that each edge appears in precisely two of the perfect matchings.

It is easy to show that this property holds for 3-edge-colorable graphs—each color class is a perfect matching, with each edge appearing in exactly one color class. Thus, if we take each color class twice, we have found the requisite 6 perfect matchings, as shown in Figure 2.4 for the 3-edge-colorable graph K_4. So, if this conjecture is to be disproved, the counterexample must be a snark. No such counterexample has yet been found—the Petersen graph with 6 perfect matchings covering each edge exactly twice is shown in Figure 2.2.

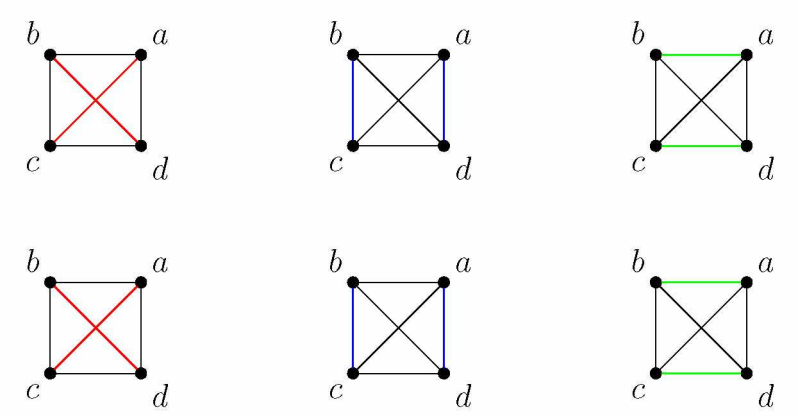

Figure 2.4: Six perfect matchings for the 3-edge-colorable graph K_4, shown in Figure 1.1.

A similar conjecture relates to *cycle double covers*. A cycle double cover (or CDC) of a graph G is a collection of cycles such that every edge of G appears in exactly two cycles. The CDC conjecture, then, is that every bridgeless graph admits a CDC.

In 1985, François Jaeger showed that in the search for a minimal counterexample to the CDC conjecture we need only consider 3-regular graphs [12]. The assumption that G is bridgeless rules out vertices of degree 1; if there exists a vertex of degree 2, we may contract that vertex and find a smaller counterexample. Moreover, if there exists a counterexample has a vertex of degree 4 or more, Jaeger showed that by modifying the edge set, one could produce a counterexample with fewer edges that is 3-regular.

Moreover, Jaeger showed that if a graph G is 3-edge-colorable, then by taking as one cycle the red and blue edges, as another the red and green edges, and as a third the blue and green edges, we can produce a CDC containing 3 cycles. Thus, if the CDC conjecture is

to be proven false, the counterexamples must once again be snarks. A CDC for the Petersen graph consisting of 6 cycles is shown in Figure 2.5 below.

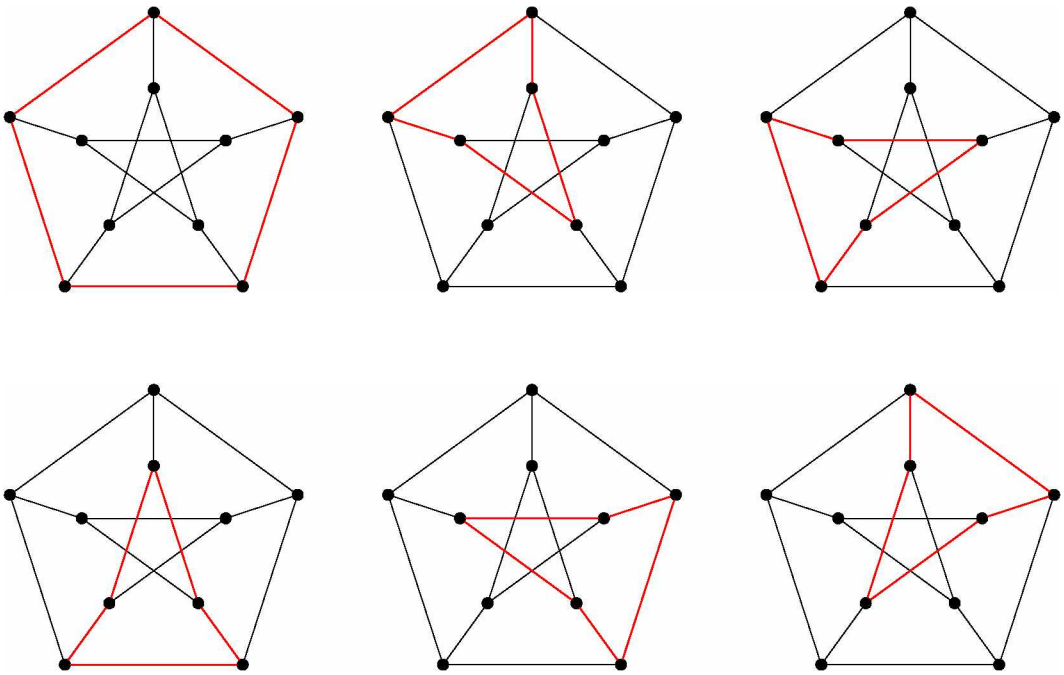

Figure 2.5: Six cycles in the Petersen graph such that each edge appears in exactly two cycles, exhibiting a CDC.

These conjectures illustrate the general trend that 3-edge-colorable cubic graphs are in some sense "nice," and so to search out the exceptional cases that may disprove conjectures, we begin with snarks.

2.3 Loupekine Snarks and k-poles

The Loupekine snarks are of particular relevance, as our construction technique grew out of Loupekine's. So, we will briefly present some of the key results and proofs from [11].

One of the key ideas used in Loupekine's construction is the notion of a *k-pole*, which is simply a graph with k *semiedges*, each of which is adjacent to only one vertex, as seen in Figure 2.6. For our purposes, multiple k-poles may be "hooked up" to one another by turning a pair of semiedges (one from each k-pole, typically) into a single edge.

Now, we may state the parity lemma, due to Blanche Descartes in [4]. The proof is a rephrasing of Descartes' proof in more modern terms.

Lemma 2 (Parity Lemma)**.** *In any proper 3-edge-coloring of a 3-regular k-pole, if n_i is the number of semiedges of color i, then*

$$n_1 \equiv n_2 \equiv n_3 \equiv k \mod 2.$$

Proof. Suppose we have some 3-regular k-pole K, which we 3-edge-color with colors red, blue, and green. Each vertex in K is incident to either a red semiedge or a red edge, and as each red edge is incident to exactly two vertices, we have that n_1 (the number of red edges) is equal to the number of vertices in K (which we call n) minus twice the number of red edges in K. Thus, n_1 has the same parity as n. By a similar argument, n_2 and n_3 also have the same parity as n, and therefore $n_1 \equiv n_2 \equiv n_3 \mod 2$. However, $n_1 + n_2 + n_3 = k$, and the sum of three odd numbers is odd, and the sum of three even numbers is even, which shows that $n_1 \equiv n_2 \equiv n_3 \equiv k \mod 2$. □

A specific example of this lemma can be seen in Figure 2.6, which is a 3-pole consisting of a triangle with a semiedge from each vertex of the triangle. To 3-edge-color the triangle, we must assign one each of red, blue, and green to the three edges of the triangle, which forces one semiedge to be red, one to be green, and one to be blue. In terms of the parity lemma, we note that because three is odd, we must have an odd number of red edges, an odd number of green edges, and an odd number of blue edges—in particular, we must have at least one of each color, as zero is even.

Loupekine observed that this lemma could be used to impose a strong condition on the semiedges of certain k-poles derived from snarks, which was presented as Lemma L in [11].

Lemma 3. *If $\{ab, bc, cb', b'a'\}$ is a path in some snark S, and A, B, C, B', A' are the corresponding semiedges in the 5-pole S' after the vertices b, c, b' are deleted from S (as shown in*

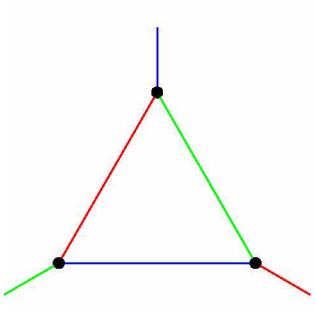

Figure 2.6: A 3-pole consisting of the triangle with a semiedge from each vertex, with a 3-edge-coloring. This illustrates the parity lemma property that in a 3-pole, each color must be represented exactly once, as zero is even while three is odd.

Figure 2.7), then in any 3-edge-coloring of S', one of the pairs of A, B and A', B' must have matching colors, and the other must have mismatched colors.

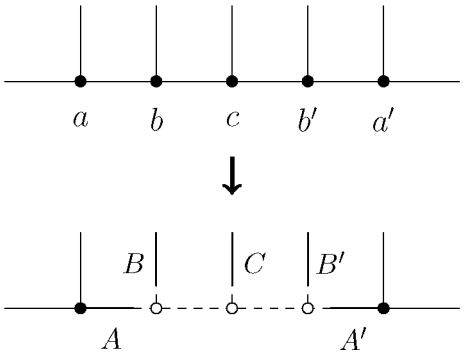

Figure 2.7: The progression from the snark S to the 5-pole S' by deleting the path $\{bc, cb'\}$ for Lemma 3.

Proof. Let S be some snark, and let $\{ab, bc, cb', b'a'\}$ be a path in S. Delete the path $\{bc, cb'\}$ from S, including the vertices b, c, and b', and name the newly created semiedges A, B, C, B', and A', as shown in Figure 2.7. We will call the resulting 5-pole S'.

Suppose we have a 3-edge-coloring for S'. Then if A and B match colors and A' and B' match colors, as in the case on the left in Figure 2.8, then there must be some color that appears on an even number of semiedges: if the color on C matches A and B or matches A' and B', then some color appears on no semiedges; if the color on C matches neither A and B nor A' and B', then the color on A and B appears an even number of times. This

contradicts the parity lemma, which states that each color must appear on an odd number of edges, as five is odd. Therefore, we cannot have that A and B match and A' and B' match.

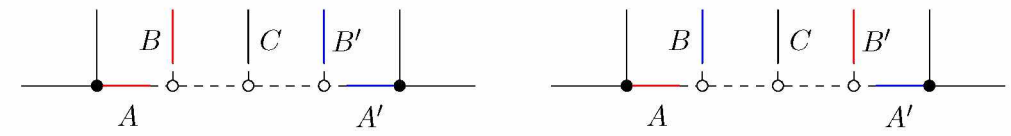

Figure 2.8: Two cases in the proof of Loupekine's Lemma that are impossible by the Parity Lemma.

So, at least one pair mismatches. Without loss of generality, assume that A and B mismatch, with A being red and B being blue. Suppose for the sake of contradiction that A' and B' also mismatch.

First, if A' and B' are also red and blue, as shown on the right in Figure 2.8, then S' has an even number of red semiedges and an even number of blue semiedges, so no matter what color C is, S' has an even number of some color of semiedges.

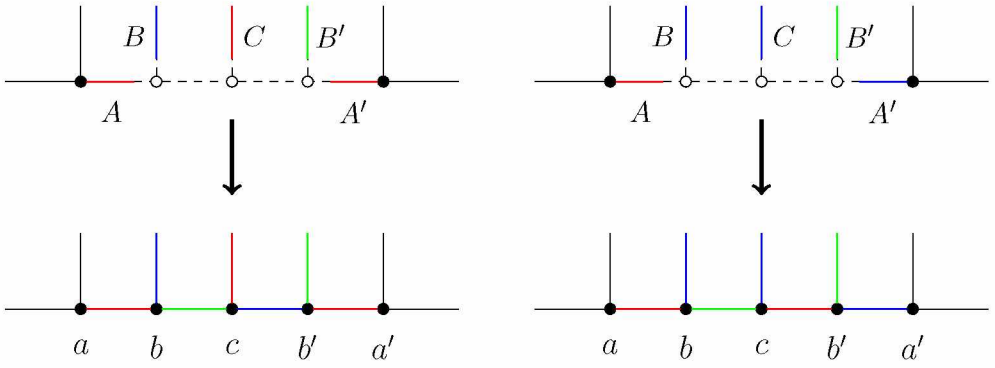

Figure 2.9: The two cases in Lemma 3 where A' and B' have mismatching colors, showing how we would obtain a 3-edge-coloring for the original snark S.

The remaining possibilities are that A' and B' are red and green, or that they are blue and green. These cases are shown in Figure 2.9. First, suppose they are red and green. Then by the Parity Lemma, C must be red to ensure we have an odd number of red edges. Give S the edge-coloring which matches S' except on the edges bc and bc'. If we color bc green and cb' blue, then we obtain a 3-edge-coloring for S, contradicting our assumption that S

was a snark.

Suppose A' and B' are blue and green. Then C must be blue, by the parity lemma. As before, color S using the 3-edge-coloring for S', and color bc green and cb' red. Again, this gives a 3-edge-coloring for S, contradicting the assumption that S was a snark. Therefore, it is impossible that A, B and A', B' both mismatch. □

Loupekine's construction technique derives immediately from this result: first, take some collection of snarks $S_1, \ldots, S_k$ and from each of them construct a 5-pole S_i' by deleting a path of length 2 as in Figure 2.7. Place these S_i' in a cycle, hooking semiedge A to A' and B to B', and finding some construction to hook the semiedges C so that the resulting graph is 3-regular. To 3-edge-color this graph, the S_i have to alternate orientation of match and mismatch in the semiedges, but when k is odd, this alternation is impossible and the resulting graph is a snark.

2.4 Conditions on Triviality

Much has been written about what can make a snark "trivial." In general, a trivial snark is a 3-regular graph that is not 3-edge-colorable for some obvious reason, such as the existence of a bridge, or because it is a simple modification of an existing snark. For a complete discussion of this topic, see Nedela and Škoviera [14], and Watkins [17].

First, we will examine the requirement that a snark be bridgeless. This condition arose out of the fact that *every* 3-regular graph with a bridge requires 4 colors to properly color its edges. This is a well-known result, sometimes included as an exercise in graph theory textbooks, but we will provide a proof here, for the sake of completeness.

Lemma 4. *If G is a 3-regular graph with a bridge, then G is not 3-edge-colorable.*

Proof. Let e be a bridge in G, and suppose, for the sake of contradiction, that there exists a proper 3-edge-coloring of G. Call the color that e receives "red." Then, because G is 3-regular and the coloring is proper with 3 colors, each vertex is incident with precisely one

edge of each color. Let G' be the subgraph of G consisting of only the red and blue edges. First, note that e is in G'. Moreover, since each vertex is incident to exactly one red edge and exactly one blue edge, every vertex is of degree 2 in G'. The subgraph G' is a collection of cycles, and therefore e lies on some cycle C in G as well. However, this means that e cannot actually be a bridge, because if we delete e, we can still get from one endpoint of e to the other by going the long way around C. This contradicts our assumption that e was a bridge. □

This condition is very easy to check—a quick visual inspection will usually immediately show whether or not a given graph has a bridge. So, we restrict the term "snark" to mean only those members of the more interesting class of bridgeless 3-regular graphs that are not 3-edge colorable.

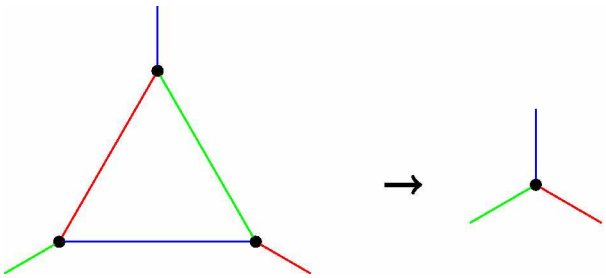

Figure 2.10: In any 3-edge-coloring, a triangle may be contracted to a point without affecting the remainder of the coloring.

One of the other conditions frequently imposed on snarks is that they must have *girth* at least 5: that is, the smallest cycle present must be of length at least 5. This condition is imposed to avoid graphs that are simply made by taking a smaller graph and adding structures that do not affect the colorability. In particular, we can see that a triangle (cycle of length 3) does not affect the colorability, because we can simply contract it to a single point: as we saw in Figure 2.6, any 3-edge-coloring of a triangle will force each of the three edges incident to the triangle to be of a distinct color, so contracting the triangle to a single point does not affect the coloring on the rest of the graph, as shown in Figure 2.10.

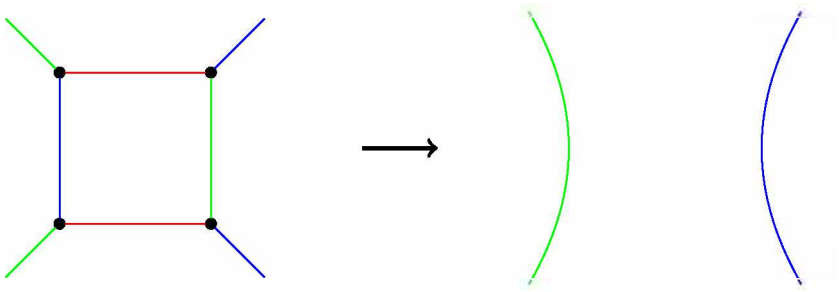

Figure 2.11: In any 3-edge-coloring, a square may be contracted to two "parallel" edges without affecting the remainder of the coloring.

A square (a cycle of length 4) can be contracted to find a smaller snark as well, although in this case the square is replaced by a pair of edges rather than a single point, as shown in Figure 2.11. However, as was pointed out in [17], *adding* a quadrilateral to a snark can turn it into a graph that is not a snark, so the situation is slightly more complicated than for triangles.

The final condition that is often imposed is that snarks must have *cyclic connectivity* of at least 4: that is, there is no set of 3 or fewer edges whose deletion breaks the graph into two or more parts, each of which contains a cycle. This condition comes from the desire to avoid graphs that are constructed by simply taking any 3-regular graph and "gluing" on a snark. The two most obvious ways of gluing correspond to cyclic connectivities 2 and 3, so non-trivial snarks are frequently considered to be those with cyclic connectivity 4 or greater.

However, even graphs that might be considered "trivial" by these conditions can have interesting properties, particularly when viewed as members of a larger family. For this reason, we will not impose these restrictions on girth or cyclic connectivity, and will use the term "snark" to refer to any bridgeless 3-regular graph that requires four colors to be properly edge-colored.

Chapter 3: The Construction of Two Families of Snarks

3.1 Voltage Graphs and Lifts

We are now almost ready begin our discussion of our new families of snarks. Following the techniques in [2], we generate our graphs as *lifts* of a particular *voltage graph*, so we begin with a discussion of that technique.

Voltage graphs and their lifts are tools used to construct drawings with rotational symmetry. For our purposes, a voltage graph is a connected *directed graph* (where edges are viewed as having direction, rather than as simply being directionless links) where each directed edge is labeled with a non-negative integer, which we view as being drawn from some voltage group $\mathbb{Z}/m\mathbb{Z}$, the cyclic group on m elements.

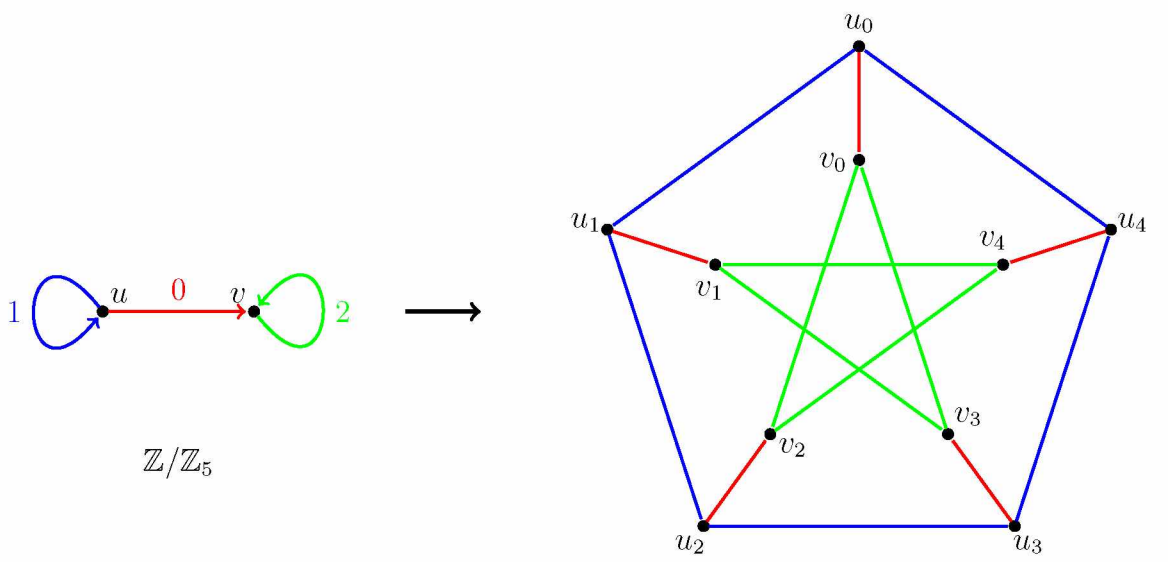

Figure 3.1: The Petersen graph as a voltage lift of the dumbbell voltage graph and voltage group $\mathbb{Z}/5\mathbb{Z}$.

A *lift* G of a voltage graph G^* with voltage group $\mathbb{Z}/m\mathbb{Z}$ is constructed as follows. First, place a copy of the vertices of some drawing of G^* arbitrarily in the plane. We label these vertices with the subscript 0, so the vertex v in G^* is labeled v_0. Then choose some point C in the plane, and for each vertex u in G^*, draw the vertices u_i as the rotation of u_0 by $\frac{2\pi i}{m}$

around C. For each directed edge from u to v with label α in G^*, we create the undirected edges u_i to $v_{i+\alpha}$ in G for each $i = 0, 1, \ldots, m-1$, where addition in the subscript is performed mod m. This construction will result in a drawing with m-fold rotational symmetry.

An example of this process is shown in Figure 3.1, where the Petersen graph is presented as the lift of a "dumbell" graph with voltage group $\mathbb{Z}/5\mathbb{Z}$. In this example, we see that because the edge from u to v in the dumbbell has label 0, we would get the same graph G if we reversed the direction of that edge. So, for simplicity of notation, when an edge in a voltage graph has a label 0, we suppress the label, and draw it as an undirected edge. For a much more thorough discussion of voltage graphs and lifts, see Gross and Tucker's book on topological graph theory [6].

3.2 The Family of Snarks, $\mathcal{F}_m$

Let L be the graph obtained by modifying the Petersen graph by subdividing the three edges incident to a single vertex and adding a vertex incident to the three new vertices. We will be following Loupekine's method and deriving a 5-pole from L, so we first show that L is a snark.

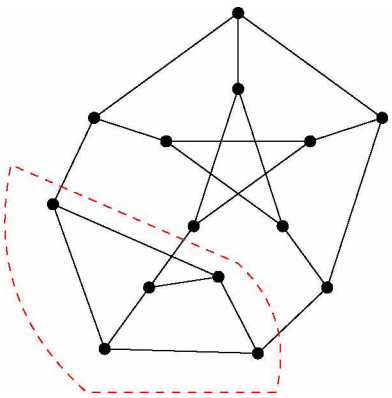

Figure 3.2: The underlying snark L. By the parity lemma, the subgraph circled in red can be contracted to a point without affecting a 3-edge-coloring of L, and when contracted this way, we recover the Petersen graph, which we know is not 3-edge-colorable.

Lemma 5. *The graph L is a snark.*

Proof. Suppose to produce a contradiction that L admits a 3-edge-coloring. By the parity lemma, the 3-pole circled in Figure 3.2 must have one edge of each color leaving it. Thus, we may contract the entire circled subgraph down to a single point without changing the 3-edge-coloring on the rest of the graph. However, this would give us a 3-edge-coloring of the Petersen graph, which is impossible. Thus, L is a snark. □

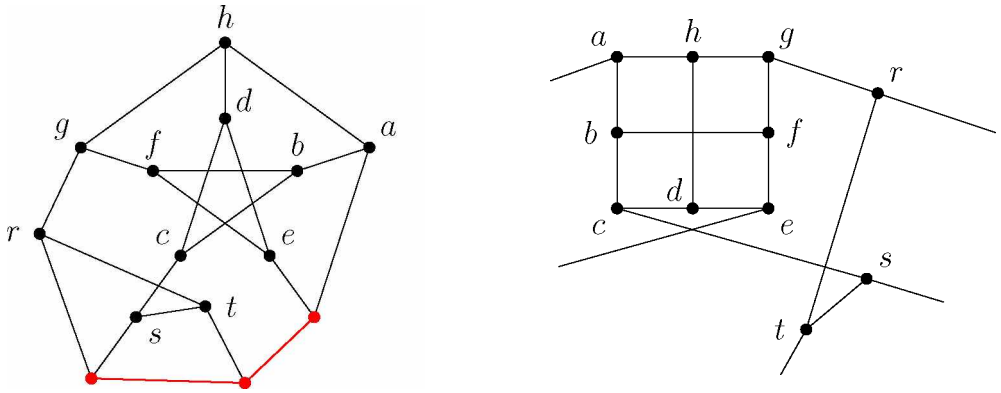

Figure 3.3: The snark L and 5-pole K that we will use to construct new snarks.

Following a method similar to Loupekine's, the graph L was converted into a 5-pole by deleting the path of length two marked in red, a process illustrated in Figure 3.3. We will refer to this particular 5-pole as K throughout the remainder of the paper. The vertices of the underlying graph and 5-pole are labeled consistently (that is, a in the underlying graph corresponds the a in the 5-pole). At times, it will be useful to refer to the subgraph consisting of the vertices $\{a, b, c, d, e, f, g, h\}$ and the edges between them, a collection we will call χ, or χ_i for the ith copy in the lift.

When converting K into a voltage graph that we will lift to our final graph, we need to ensure that the final graph remains 3-regular. Thus, we introduce a vertex ℓ in the voltage graph that is incident to t and has a directed loop with label p_3. We replace the semiedges incident to a and r with an arrow from r to i with label p_1, and the semiedges incident to c and s with a directed edge from c to s with label p_2. The final voltage graph, which we will call G is shown in Figure 3.4.

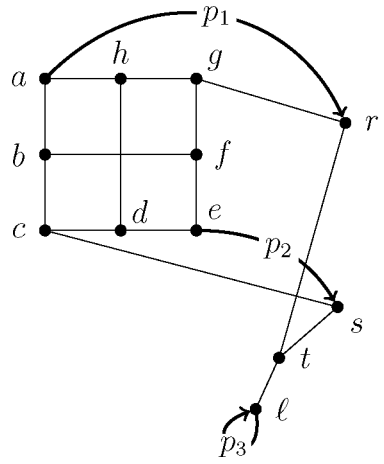

Figure 3.4: The voltage graph we use to generate new snarks, constructed by replacing pairs of semiedges in K with arrows, adding the vertex ℓ at the end of the semiedge incident with t, and adding the directed loop at ℓ.

We also introduce compact notation for the parameters of the lift. By the notation $G(m, p_1, p_2, p_3)$, we mean the graph that is the lift of G, where the parameters p_1, p_2, and p_3 are viewed as being elements of $\mathbb{Z}/m\mathbb{Z}$. We will be primarily concerned with the examples where $p_1 = p_2 = p_3 = 1$, so we will use $\mathcal{F}_m$ to refer to the graph $G(m, 1, 1, 1)$ for $m \geq 3$. For $m = 1$ and 2, we get loops or doubled edges in the lift, a situation which we would prefer to avoid, so we will restrict our consideration to $m \geq 3$.

As an example, the graph $\mathcal{F}_4$ is shown in Figure 3.5, with a single copy of K from Figure 3.3 circled in red to illustrate the construction technique. A natural drawing of this graph is in three dimensions, as shown in Figure 3.6.

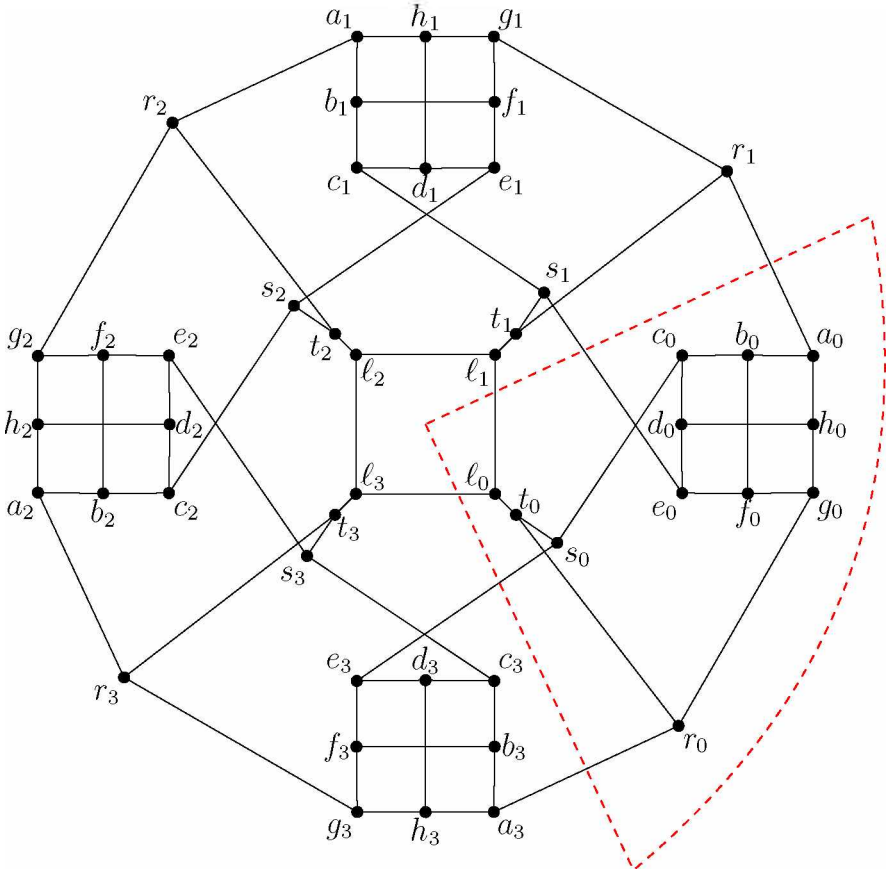

Figure 3.5: The graph $\mathcal{F}_4$, with vertex labels. The 0^{th} copy of the 5-pole K from Figure 3.3 is circled.

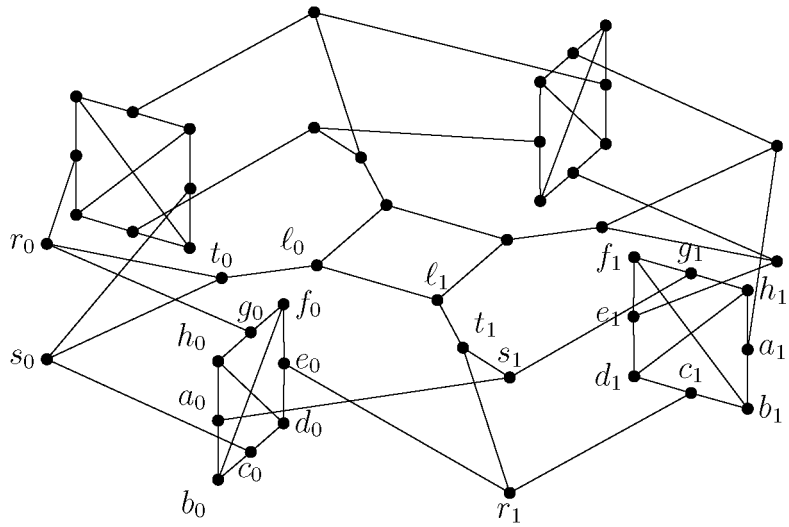

Figure 3.6: A projection of a three-dimensional drawing of the graph $\mathcal{F}_4$, showing only the 0 and 1 labels, for legibility.

3.3 A Second Family of Snarks, $\mathcal{R}_m$

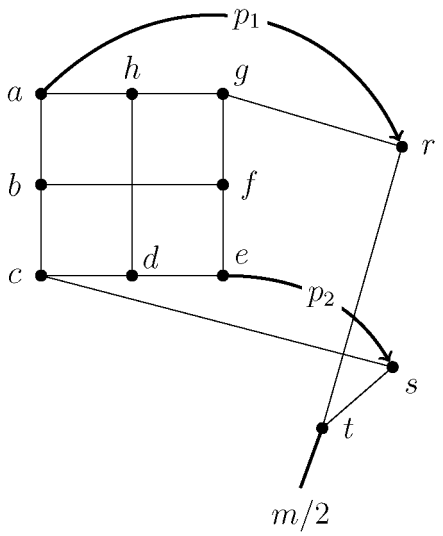

Figure 3.7: The voltage graph, G_d, for the modified graphs with diameters, with voltage group $\mathbb{Z}/m\mathbb{Z}$ for even m. The semiedge with label $m/2$ is treated like a loop, except that if the edge it would create in the lift is already present, it is not doubled.

There is a modification of the construction technique which provides even smaller examples. For even m, rather than linking up the points ℓ_i in a central cycle, we instead delete the points ℓ_i and connect k_i to $k_{i+m/2}$. That is, we create diameters. The voltage graph G_d for this construction is shown in Figure 3.7. By the notation $G_d(m, p_1, p_2)$ we mean the lift of G_d, where the parameters p_1 and p_2 are viewed as elements of $\mathbb{Z}/m\mathbb{Z}$. We will use $\mathcal{R}_m$ to denote the lift $G_d(m, 1, 1)$. An example, $\mathcal{R}_4$, is shown in Figure 3.8. The snark with the fewest number of vertices of any of the $\mathcal{F}_m$ or $\mathcal{R}_m$ is $\mathcal{R}_2$ on 22 vertices, and is shown in Figure 3.9.

This small snark $\mathcal{R}_2$ is one of the 20 snarks on 22 vertices enumerated in the snarks listing of the House of Graphs online database [3]. However, it is not one of the two famous Loupekine snarks on 22 vertices, as each of those graphs has cyclic connectivity 5, while $\mathcal{R}_2$ has cyclic connectivity 4, as do all the graphs $\mathcal{F}_m$ and $\mathcal{R}_m$.

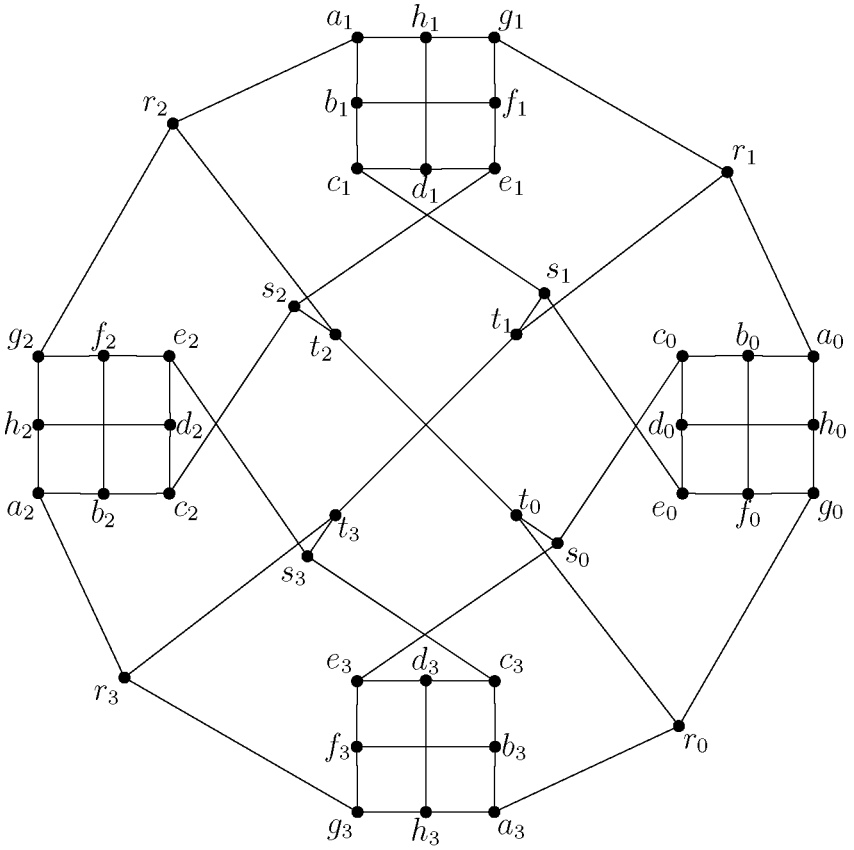

Figure 3.8: The graph $\mathcal{R}_4$ on 44 vertices.

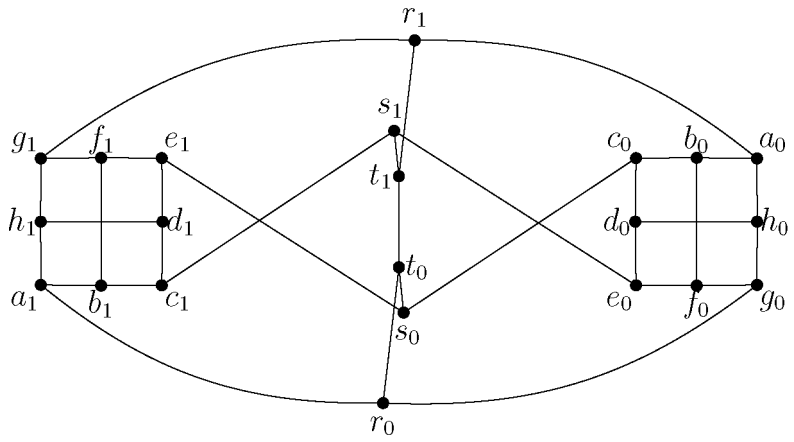

Figure 3.9: The graph $\mathcal{R}_2$ on 22 vertices.

Chapter 4: Results

4.1 Proof that the graphs $\mathcal{F}_m$ and $\mathcal{R}_m$ are Snarks

We begin with the first major result of this paper: that the graphs we have constructed are, in fact, snarks.

Theorem 1. *The graph $\mathcal{F}_m$ is a snark for all $m \geq 3$.*

Proof. We begin by applying the Parity Lemma to the 5-pole K to see that we must have precisely three semiedges of one color and one of each of the other two colors in any 3-coloring. As we saw in Loupekine's Lemma, (Lemma 3 in this text), we must have exactly one of the pairs of A, B and A', B' matching, and the other mismatching.

In our case, we let the color that appears on three semiedges be known as red, with the other two colors being green and blue. There are $\binom{5}{3} = 10$ possibilities for which of the semiedges receive color red, and as each of the other colors appear on precisely one semiedge, they are interchangable. Thus, the 10 choices of which three edges are red covers all distinct choices for the semiedges. The three choices for which it is possible to fully 3-color K are shown below in Figure 4.1, and the remaining choices are shown in Figures 4.2, 4.3, and 4.4.

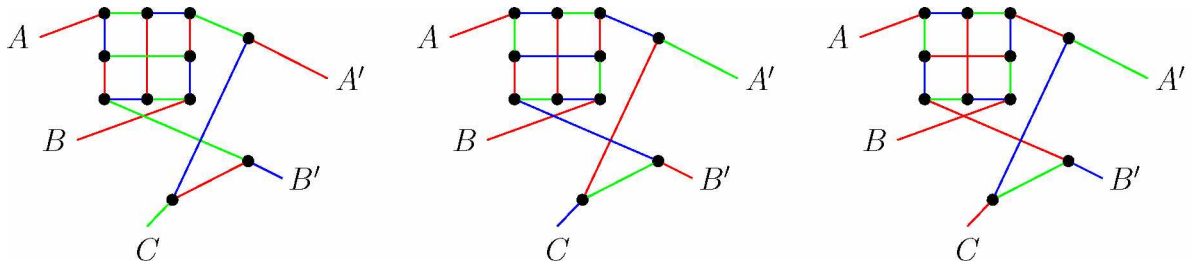

Figure 4.1: The three choices of colors for the semiedges of the 5-pole K from Figure 3.3 that lead to valid 3-edge-colorings.

If we examine the three possible colorings of K in Figure 4.1, we observe that in each case, the semiedges A and B must receive the same color, while the semiedges A' and B' must mismatch. Thus, we have, in a sense, an *oriented* Loupekine's lemma. We are not aware of

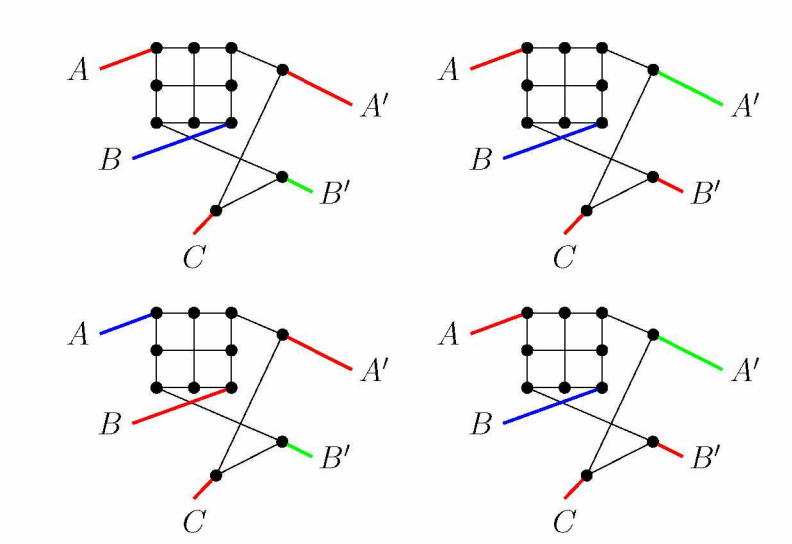

Figure 4.2: Four possible assignments of colors to semiedges in the 5-pole K that are impossible by Loupekine's Lemma, as both A and B and A' and B' mismatch.

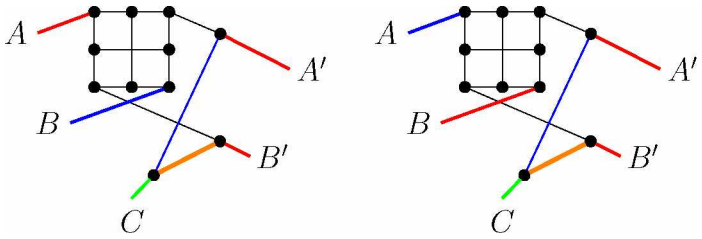

Figure 4.3: Two assignments of colors to semiedges in K that don't lead to 3-edge-colorings, with the thick orange edge indicating the point where issues with 3-edge-coloring arise.

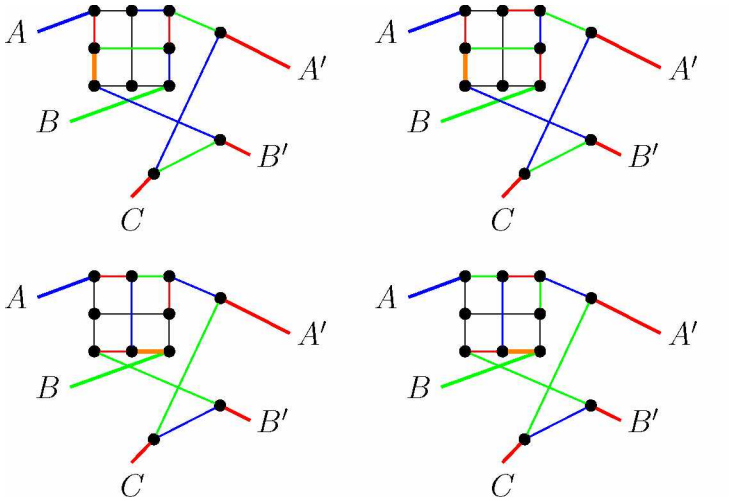

Figure 4.4: The final possible assignment of colors to semiedges in K, with four attempts to 3-edge-color K, exhausting all free choices. The thick orange edge indicates where issues with 3-edge-coloring arise.

this notion of graphs with an enforced orientation on possible 3-edge-colorings being used to construct snarks previously, and a possibly fruitful open line of questioning is whether there are other graphs that have this property.

In $\mathcal{F}_m$, the edges a_0r_1 and e_0s_1 must be connecting K_0 to K_1. From the perspective of K_0, these are the semiedges A and B, and thus must have matching colors in any 3-edge-coloring of K_0. However, from the perspective of K_1, these are the edges A' and B', and thus must have mismatching colors in any 3-edge-coloring. These requirements conflict, so there is no way to 3-edge-color $\mathcal{F}_m$. □

In this proof, we only used the fact that $p_1 = p_2$, so the edges $a_0r_{p_1}$ and $e_0s_{p_2}$ both connect the same two copies of K (in $\mathcal{F}_m$, the copies are K_0 and K_1). So, we have an immediate corollary.

Corollary 1. *The graph $G(m, p_1, p_2, p_3)$ is a snark if $p_1 = p_2$ for $m \geq 3$.*

Moreover, the inner cycle was immaterial to the proof above, so the equivalent results for the second family with diameters are an immediate corollary.

Corollary 2. *The graph $\mathcal{R}_m$ is a snark for $m \geq 2$. More generally, $G_d(m, p_1, p_2)$ is a snark if $p_1 = p_2$ for $m \geq 2$.*

4.2 Interpreting $\mathcal{F}_m$ and $\mathcal{R}_m$ as Blowup Graphs

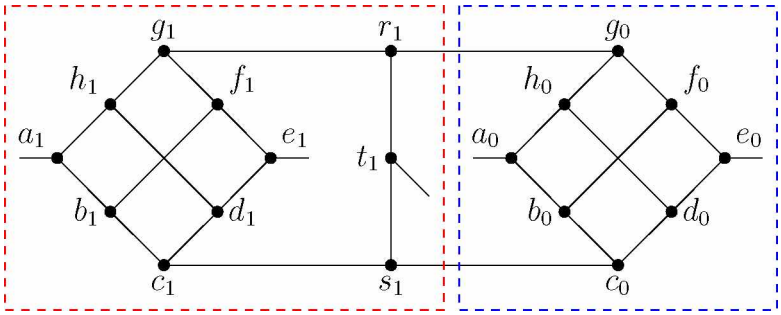

Figure 4.5: The 5-pole H_2 from [8], with labels viewed as K_1 (circled in red) adjoined with χ_0 (circled in blue).

After having proved the result above, we realized that this could be seen as a consequence of a result from Jonas Hägglund's 2016 paper [8]. In that paper, Hägglund showed that the 5-pole H_2, shown in Figure 4.5, is not 3-colorable, and thus any graph containing H_2 as a subgraph must also be non-3-colorable.

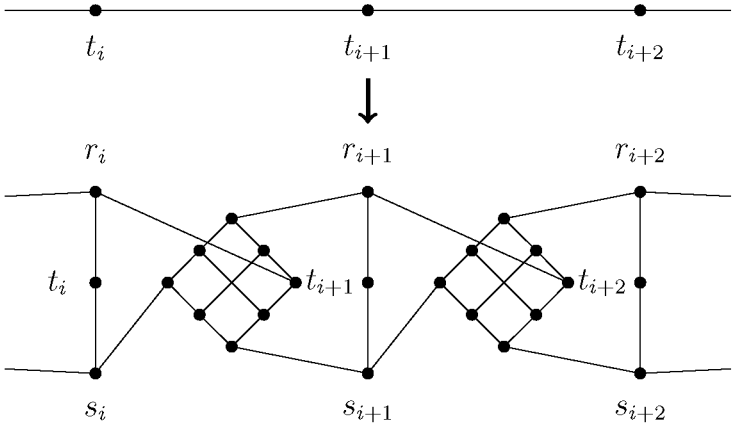

Figure 4.6: The blowup technique from [8].

We can see the 5-pole H_2 as a single copy of our 5-pole K with an extra copy of the subgraph χ attached (recall that χ is the subgraph of K containing only the 8 vertices in the "grid"). So, the graphs $\mathcal{F}_m$ and $\mathcal{R}_m$ contain H_2 as a subgraph. Moreover, $\mathcal{F}_m$ and $\mathcal{R}_m$ can be seen as special cases of the *blowup* construction introduced by Hägglund in [8].

The blowup construction can be summarized as follows: one takes any 2-edge-connected cubic graph with a 2-regular subgraph D. Let $C = (k_0, k_1, \ldots, k_{n-1})$ be a cycle in D; then we delete all the edges in C, add two vertices i_i and j_i adjacent to each k_i, and add a copy of

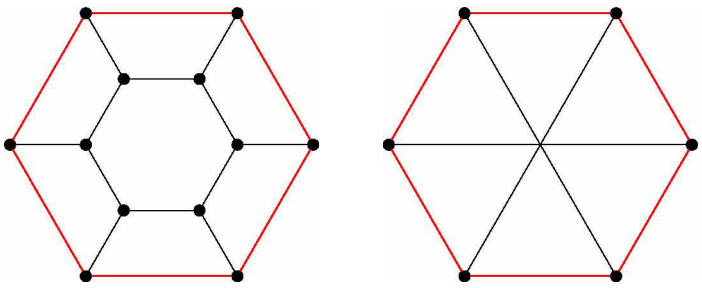

Figure 4.7: The prism with 6-fold rotational symmetry (left) and a 6-cycle with diameters (right). The cycle around which we perform the blowup is indicated in red.

the "grid graph" χ_i between the pairs of vertices $\{i_i, j_i\}$ and $\{i_{i+1}, j_{i+1}\}$, as shown in Figure 4.6.

It follows that $\mathcal{F}_m$ is the blowup of the prism with m-fold rotational symmetry, where the blowup is performed around the outer m-cycle of the prism, while for even m, $\mathcal{R}_m$ is the blowup of an m-cycle with diameters added. Examples with $m = 6$ for both these cases are shown in Figure 4.7; the cycle C around which the blowup would be performed is shown in red.

4.3 Automorphism Group

The automorphism group of snarks $\mathcal{F}_m$ are large, as we will show by demonstrating a number of distinct automorphisms. First, because we constructed $\mathcal{F}_m$ as the lift of a voltage graph, the principal drawing of $\mathcal{F}_m$ has rotational symmetry of order m, giving us m distinct rotational automorphisms. We will use the notation τ to mean rotation by $\frac{2\pi}{m}$ around the center of the drawing, and also the corresponding combinatorial automorphism.

Next, we show that G has dihedral symmetry, as shown in Figures 4.8 and 4.9. While these are not quite geometric reflections of the given two-dimensional drawing, this is only due to the points r_i and s_i being shifted slightly for clarity, a distinction that does not affect the graph automorphism. In fact, the natural embedding of $\mathcal{F}_m$ is in three dimensions, as shown in Figure 3.6, where the combinatorial automorphism is genuinely reflection through a plane. We let σ_0 represent combinatorial "reflection" across the mirror passing through d_0.

Note that the automorphism group generated by τ and σ_0 is precisely D_m, the dihedral group of order $2m$, and D_m is therefore a subgroup of $\mathrm{Aut}(\mathcal{F}_m)$.

However, there are more automorphisms in $\mathrm{Aut}(\mathcal{F}_m)$. For each i, there is an automorphism, which we will call γ_i, or a "bridge flip" that performs the following vertex maps and

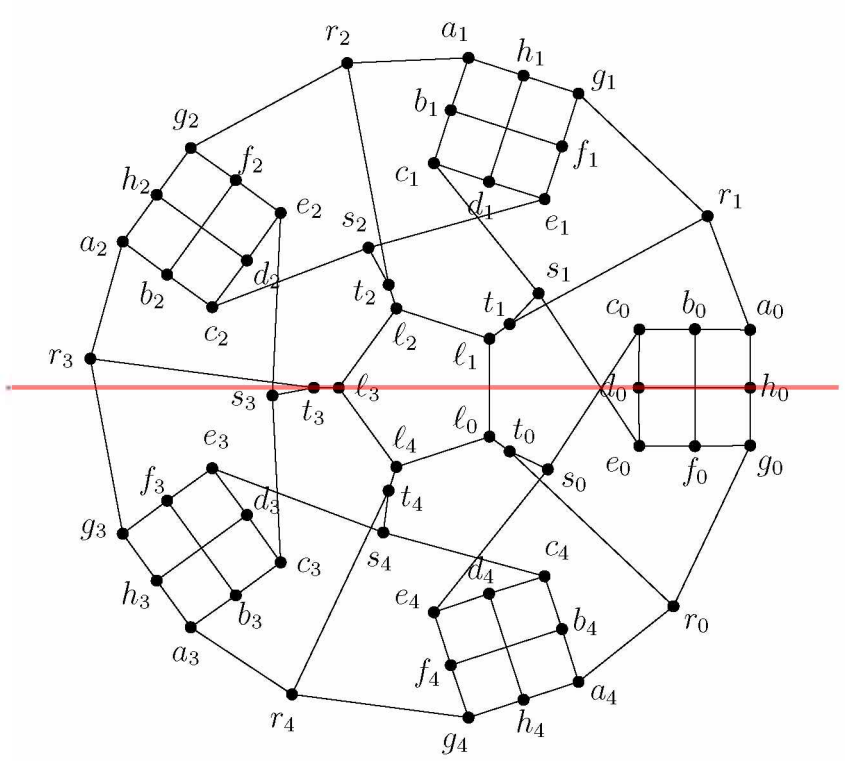

Figure 4.8: The graph $\mathcal{F}_5$. The red line acts as a mirror, fixing the points $\ell_3, t_3, s_3, r_3, d_0$ and h_0, which corresponds to the automorphism σ_0.

fixes all the other vertices:

$$i_i \longleftrightarrow j_i \qquad b_i \longleftrightarrow h_i \qquad c_i \longleftrightarrow g_i \qquad d_i \longleftrightarrow f_i$$

$$b_{i-1} \longleftrightarrow d_{i-1} \qquad a_{i-1} \longleftrightarrow e_{i-1} \qquad h_{i-1} \longleftrightarrow f_{i-1}$$

An example of γ_1 on $\mathcal{F}_5$ is shown in Figure 4.10.

Note that each γ_i is of order 2, and there are m distinct γ_i, so $\mathrm{Aut}(\mathcal{F}_m)$ has m distinct subgroups of order 2, in addition to the subgroup isomorphic to D_m. Thus, $\mathrm{Aut}(\mathcal{F}_m)$ has order at least $(2m)(2^m) = 2^{m+1}m$. We will now show that τ, σ_0, and the γ_i in fact generate *all* the automorphisms of $\mathcal{F}_m$.

Theorem 2. *The order of the automorphism group of $\mathcal{F}_m$ is precisely $2^{m+1}m$.*

Proof. We have already shown that $|\mathrm{Aut}(\mathcal{F}_m)| \geq 2^{m+1}m$, so we need only show the opposite inequality. To do so, we will argue that when determining an arbitrary automorphism,

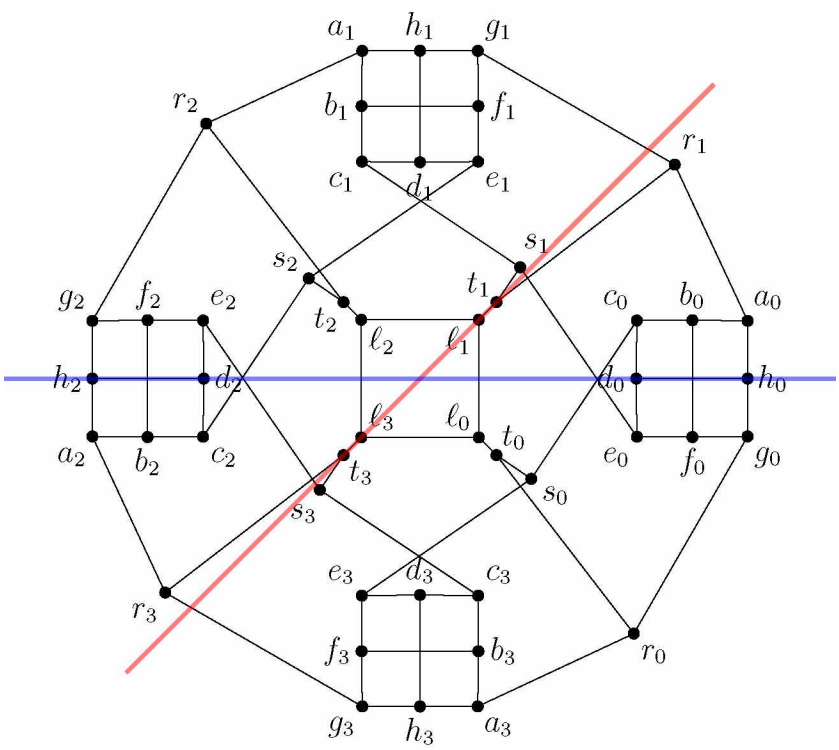

Figure 4.9: The graph $\mathcal{F}_4$. The blue line acts as a mirror, fixing d_0, h_0, d_2, and h_2, and corresponds to the automorphism σ_0. The red line also acts as a mirror, fixing the points $\ell_1, t_1, s_1, r_1, \ell_3, t_3, s_3$, and r_3, which corresponds to the automorphism σ_1.

there are only so many choices one can make, where each choice corresponds to a distinct automorphism.

We begin by defining the following collections of vertices, which are shown in Figure 4.11:

$$U = \{a_i, c_i, e_i, g_i\}_{0 \le i \le m-1}$$

$$V = \{b_i, d_i, f_i, h_i\}_{0 \le i \le m-1}$$

$$X = \{r_i, s_i\}_{0 \le i \le m-1}$$

$$Y = \{t_i\}_{0 \le i \le m-1}$$

$$Z = \{\ell_i\}_{0 \le i \le m-1}.$$

We will show that each of these sets is in fact an orbit under the automorphism group of $\mathcal{F}_m$. First, we claim that under τ, γ_i and σ_i, we can map any vertex in U to any other

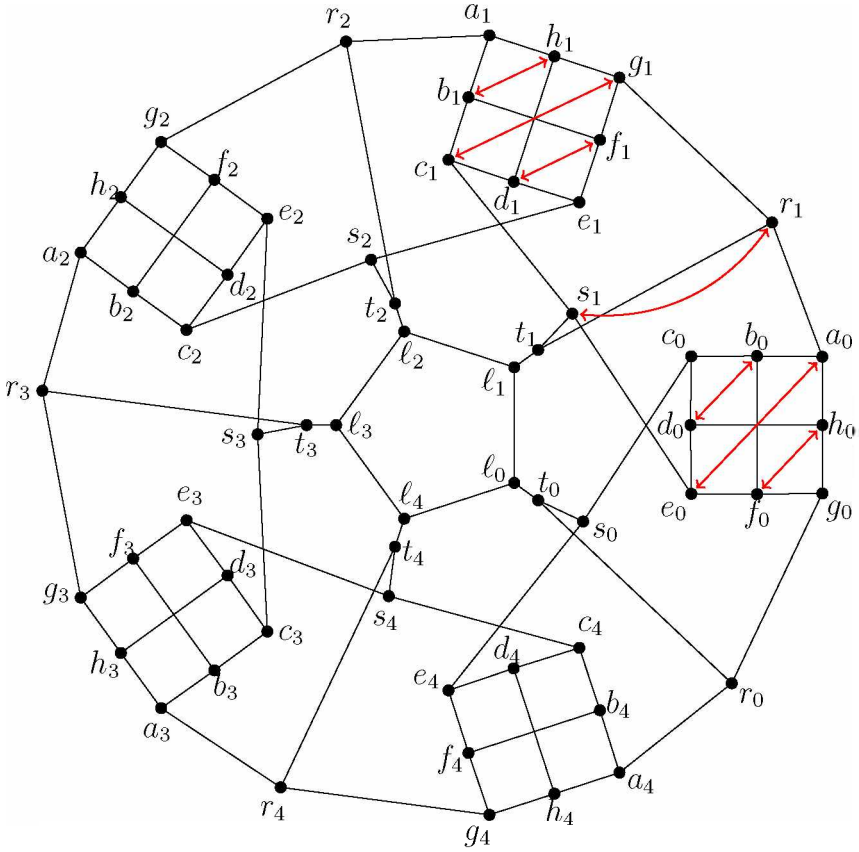

Figure 4.10: The graph $\mathcal{F}_5$. Performing the swaps indicated by the red double-headed arrows (i.e., $b_1 \mapsto h_1$, $h_1 \mapsto b_1$, $c_1 \mapsto g_1$, $g_1 \mapsto c_1$, etc.) gives the bridge flip γ_1.

vertex in U, and similarly for vertices in V, X, Y, and Z. For vertices $u, v \in Y$, we can easily map u to v by τ^i for some i, and similarly for vertices in Z. For vertices in X, we may need to compose γ_i with τ^k for some i, k, but the map is still clear. For vertices in U, we note that σ_0 interchanges a_0 with g_0 and c_0 with e_0, while γ_1 interchanges a_0 with e_0. Thus, as shown in Figure 4.12, by some composition of σ_0 and γ_1 it is possible to map any member of $\{a_0, c_0, e_0, g_0\}$ to any other, and the remainder of U follows by composition with τ^i. Showing that we map any vertex in V to any other follows similarly.

As an example, suppose we want to map c_0 to a_2. First, we apply σ_0 to map c_0 to e_0. Then, applying γ_1, we map e_0 to a_0. Finally, we apply τ^2, taking a_0 to a_2. Thus, $\tau^2 \circ \gamma_1 \circ \sigma_0$ is an automorphism of $\mathcal{F}_m$ that takes c_0 to a_2.

Now we will show that under any automorphism, a vertex in U *must* go to another vertex

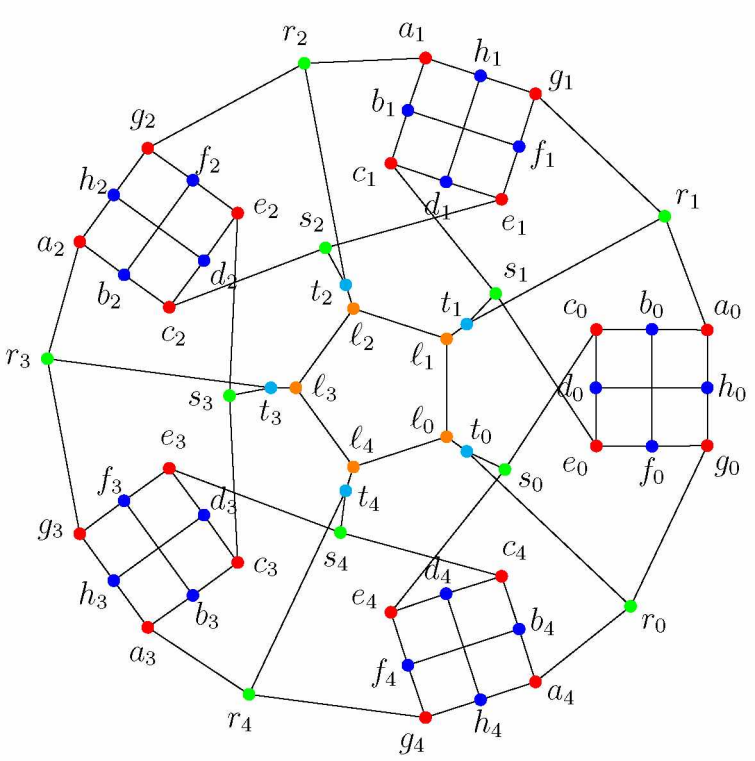

Figure 4.11: The graph $\mathcal{F}_5$, with the points in U highlighted in red, the points in V highlighed in blue, the points in X highlighted in green, the points in Y highlighted in cyan, and the points in Z highlighted in orange.

in U, and similarly for the other classes.

First, we observe that every vertex in U lies on precisely 2 five-cycles, while each vertex in V lies on precisely 3 five-cycles, as shown in Figure 4.13. Thus, no vertex in U may be mapped to a vertex in V, and because each vertex in one of the sets X, Y, Z lies on at most one 5-cycle, U and V are distinct orbits under $\mathrm{Aut}(\mathcal{F}_m)$.

Next, we observe that each vertex in X is adjacent to some vertex in U, while no vertex in Y or Z is adjacent to a vertex in U. Moreover, each vertex in Y is adjacent to a vertex in X, which no vertex in Z is. Thus, X, Y, and Z are each distinct orbits under any automorphism of $\mathcal{F}_m$.

By counting the number of free choices we have in mapping the orbits U, V, X, Y, Z to themselves, we will establish an upper bound on the number of automorphisms in $\mathrm{Aut}(\mathcal{F}_m)$. So, let α be any automorphism of $\mathcal{F}_m$. Then, because the orbit Z contains only the vertices

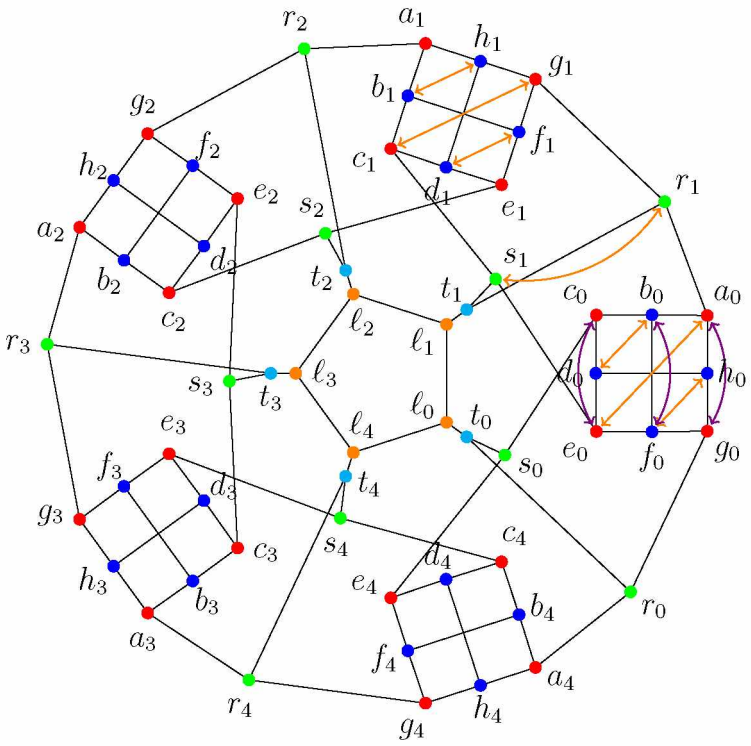

Figure 4.12: The graph $\mathcal{F}_5$. The effects of σ_0 on K_0 are represented by purple arrows while γ_1 is represented by orange arrows. Under some composition of these two automorphisms, it is possible to map any red vertex in K_0 (that is, a_0, c_0, e_0, or g_0) to any other red vertex in K_0, and similarly for the blue vertices.

$\{\ell_i\}_{0\leq i\leq m-1}$, we know that $\alpha(\ell_0) = \ell_n$ for some n, for which we have m choices. Once ℓ_0 has been mapped to some ℓ_n, then ℓ_1 must be mapped to an ℓ vertex adjacent to ℓ_n: that is $\alpha(\ell_n) = \ell_{n+1}$ or ℓ_{n-1}, for an additional two choices. This choice also determines $\alpha(\ell_i)$ for all $i = 0, 1, \ldots, m-1$. Moreover, as t_0 is the unique vertex in Y adjacent to ℓ_0, we must have that $\alpha(t_0) = t_n$, and similarly for all the vertices in Y.

Next, notice that while α must map r_0 to a vertex in X adjacent to $\alpha(t_0) = t_n$, there are two choices: $\alpha(r_0) = r_n$ or s_n. This choice naturally determines where s_0 is mapped as well. So, for each r_i, there are an additional two choices, giving us a total of 2^m choices for how α maps the vertices in X.

Finally, notice that the index 0 "grid graph," χ_0, has edges only within itself and to the two pairs of vertices in X on either side, in this case r_0 and s_0 on one side and r_1 and s_1 on the other. Thus, χ_0 must be mapped as a unit, and it must be mapped to the grid graph

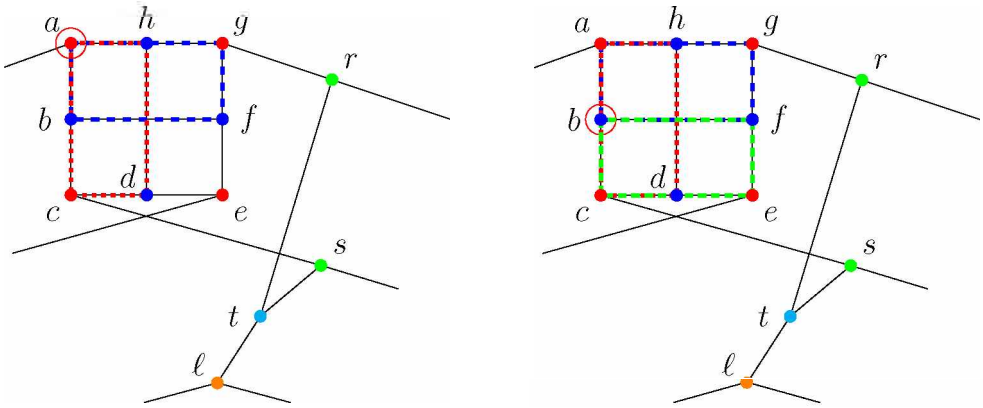

Figure 4.13: Two copies of K, with the two cycles through a marked in red and blue on the left, and the three three cycles through b marked in red, blue, and green on the right.

between $\alpha(r_0)$ and $\alpha(r_1)$. Moreover, as r_0 is adjacent only to g_0 in the index 0 grid graph, $\alpha(g_0)$ is fully determined, and similarly for $\alpha(a_0)$, $\alpha(c_0)$, and $\alpha(e_0)$. With the corners of $\alpha(\chi_0)$ determined, the action of α on the internal vertices is also fully determined.

Looking back at the previous paragraphs, we notice that our free choices were in determining where ℓ_0 was mapped, where we had m choices; in determining where ℓ_1 was mapped, where we had two choices; and in determining the action of α on the vertices in X, where we had 2^m choices. Thus, we had a total of $2^{m+1}m$ choices, which corresponds to the upper bound $|\operatorname{Aut}(\mathcal{F}_m)| \leq 2^{m+1}m$. However, we had already exhibited automorphisms showing that $|\operatorname{Aut}(\mathcal{F}_m)| \geq 2^{m+1}m$, so $|\operatorname{Aut}(\mathcal{F}_m)| = 2^{m+1}m$. □

As before, we would like to prove a similar result about the automorphism group of graphs in $\mathcal{F}_d$.

Theorem 3. *The order of the automorphism group of $\mathcal{R}_m$ is precisely $2^{m+1}m$.*

Proof. We first observe that all of the automorphisms τ_i, σ, and γ_i that we discussed in the context of $\mathcal{F}_m$ are also automorphisms of $\mathcal{R}_m$, so the order of $\operatorname{Aut}(\mathcal{R}_m)$ is at least $2^{m+1}m$.

We follow the same fundamental pattern as our proof of Theorem 2, in that we will argue that when determining an arbitrary automorphism, there are restrictions on the number of choices one can make.

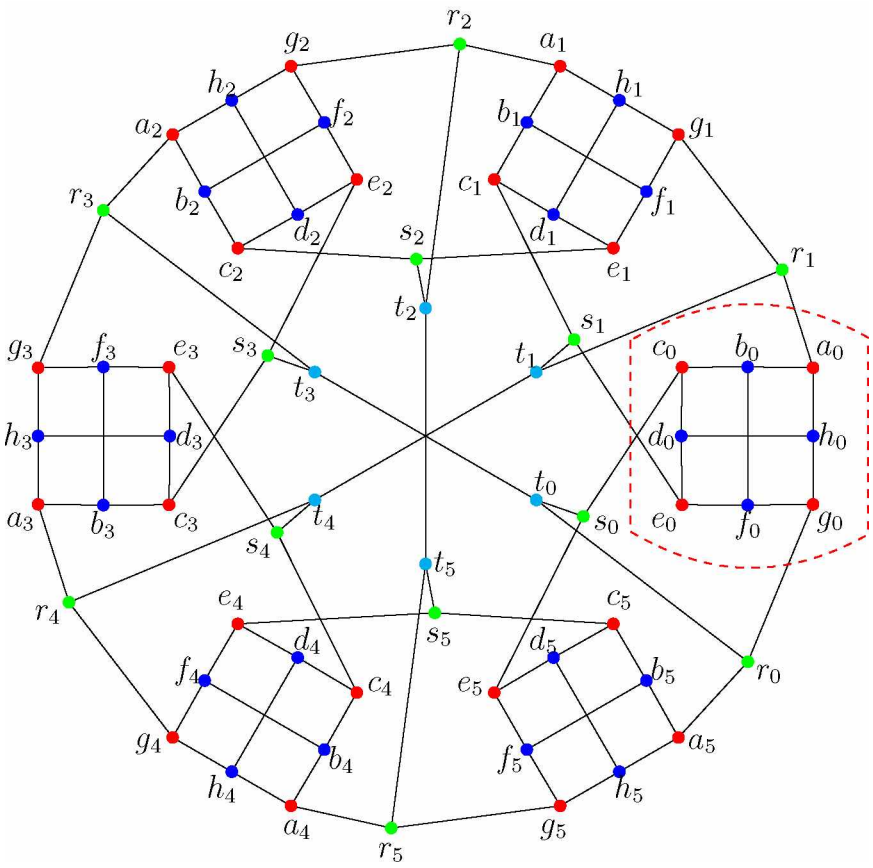

Figure 4.14: The graph $\mathcal{R}_6$, with the points in U highlighted in red, the points in V highlighed in blue, the points in X highlighted in green, and the points in Y highlighted in cyan. The grid graph χ_0 is outlined with a dashed red line.

As in Theorem 2, we define the sets

$$U = \{a_i, c_i, e_i, g_i\}_{0 \leq i \leq m-1}$$

$$V = \{b_i, d_i, f_i, h_i\}_{0 \leq i \leq m-1}$$

$$X = \{r_i, s_i\}_{0 \leq i \leq m-1}$$

$$Y = \{t_i\}_{0 \leq i \leq m-1},$$

each of which is shown as a set of vertices of the same color in Figure 4.14. By a similar proof as for $\mathcal{F}_m$, each of the U, V, X, and Y forms a distinct orbit. Thus, if α is any automorphism

of G, $\alpha(t_0) = t_n$ for some n with $0 \leq n \leq m-1$. Thus, we have m choices for where n is mapped.

As before, we have two choices for where to map r_0 and r_0 - either $\alpha(r_0) = r_n$ (and thus $\alpha(s_0) = s_k$) or $\alpha(r_0) = s_n$ (and $\alpha(s_0) = r_n$), which gives us an additional two choices.

We noted previously that the grid graph χ_0 (circled with a dashed red line in Figure 4.14) must be mapped as a unit under α. Moreover, as $\alpha(\chi_0)$ must have edges to $\alpha(r_0)$ and $\alpha(s_0)$, χ_0 must be mapped to either χ_n or χ_{n-1}, for an additional 2 choices. This is essentially the same argument as was presented above for the vertices ℓ_i in Z; however, in this case we are mapping entire subgraphs χ_i rather than vertices. Note that at this point, we have not determined where in $\alpha(\chi_0)$ individual vertices are being mapped, just where the subgraph as a whole has been mapped.

Now, the vertices r_1 and s_1 have edges to χ_0, so they must be mapped into the two vertices in X that have edges into $\alpha(\chi_0)$ remaining after we have mapped r_0 and s_0. As before, there are two choices for where r_1 goes. This fixes $\alpha(t_1)$, since it is the vertex in Y adjacent to $\alpha(r_1)$ and $\alpha(s_1)$. Moreover, once we have chosen how to map r_1 and s_1, we have fully determined the behavior of the map on χ_0, in between r_0 and r_1, as in the proof for $\mathcal{F}_m$.

The grid graph χ_1 has edges to the vertices r_1 and s_1, so its location under α is determined by choices already made. Proceeding around the graph, we find that for each pair of vertices r_k and s_k, we have two choices, and that these choices fully determine where α maps the U, V, X and Y vertices.

In total, we had m choices for where to map t_0, 2 choices for which side of the vertices $\alpha(r_0)$ and $\alpha(s_0)$ to map χ_0 to, and then 2^m choices for how to map the vertices in X. Thus, there are at most $2^{m+1}m$ choices, which as in Theorem 2 is enough to establish the result that $|\operatorname{Aut}(\mathcal{R}_m)| = 2^{m+1}m$. □

4.4 Oddness

To define the notion of the oddness of a graph, we first need the notion of a 2-factor: a *2-factor* of a graph is a collection of disjoint cycles (i.e., having no edge or vertex in common) such that every vertex in the graph appears in exactly one cycle. The *oddness* of a graph G is defined as

$$\omega(G) = \min_{\text{2-factors } M \text{ of } G} \{\text{number of odd cycles in } M\}.$$

As an example, a 2-factor of the Petersen graph is marked in red in Figure 4.15, composed of two 5-cycles. It turns out that this is the minimum number of odd cycles we can get in any 2-factor, so the oddness of the Petersen graph is 2.

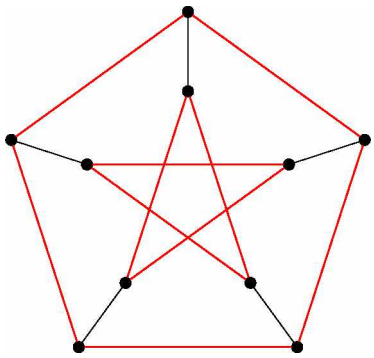

Figure 4.15: The Petersen graph, with a 2-factor composed of 2 odd cycles marked in red. As this is the minimum number of odd cycles in any 2-factor, the Petersen graph has oddness 2.

There is an immediate connection between oddness and snarks, in that a bridgeless 3-regular graph is a snark if and only if it has oddness not equal to 0.

More generally, as discussed in [13], the oddness of a graph can be seen as a measure of its uncolorability, because deleting a single vertex from each odd cycle in a 2-factor yields a 3-colorable graph. It is not surprising, then, that snarks of low oddness behave in some sense "almost" like a 3-colorable graph. In particular, some of the conjectures in graph theory that look to snarks for counterexamples have been shown to hold for snarks of low oddness. For example, in 1995, Huck and Kochol showed in [9] that the 5-cycle double cover conjecture

was satisfied for snarks of oddness exactly 2, while in 2004 Häggkvist and McGuinness proved in [7] that a similar result for holds snarks of oddness exactly 4. So, snarks of large oddness are of interest.

In [8], Hägglund showed that a lower bound for the oddness of snarks constructed via the blowup construction was $\lceil \frac{m}{2} \rceil$, where m is the length of the cycle around which the blowup is performed. In the case of the construction presented in this paper, m is in fact the order of rotational symmetry, by construction.

We can improve this lower bound slightly by considering cases on m. The following is a well-known result, which we re-prove here.

Lemma 6. *For any 3-regular graph G, the oddness, $\omega(G)$, is even.*

Proof. We observe first that by the Handshake Lemma, $2e = 3v$, where e is the number of edges in G and v is the number of vertices. However, this implies that $3v$ is even, and therefore that G has an even number of vertices.

Now suppose to produce a contradiction that $\omega(G)$ is odd. Then there exists a 2-factor H of G with $\omega(G)$ odd cycles. Because $\omega(G)$ is odd, the odd cycles of H together contain an odd number of vertices. However, because G contains an even number of vertices, there remains an odd number of vertices to be spanned by the even cycles of H, which is impossible. Thus, $\omega(G)$ must be even. □

This gives us an immediate improvement on the lower bound from Hägglund, in that if $\lceil \frac{m}{2} \rceil$ is odd, then by Lemma 6, the lower bound on the oddness is in fact $\lceil \frac{m}{2} \rceil + 1$. For even m, $\frac{m}{2}$ will be odd precisely when $m \equiv 2 \mod 4$, which suggests considering $m \mod 4$ in general.

We first consider the cases where m is even, allowing us to dispense with the ceiling notation. If $m \equiv 0 \mod 4$, then $4 \,|\, m$, so $\frac{m}{2}$ is even, and $\omega(\mathcal{F}_m) \geq \frac{m}{2}$. If $m \equiv 2 \mod 4$, then $2 \,|\, m$, but 4 does not divide m, so $\frac{m}{2}$ is odd, and $\omega(\mathcal{F}_m) \geq \frac{m}{2} + 1$.

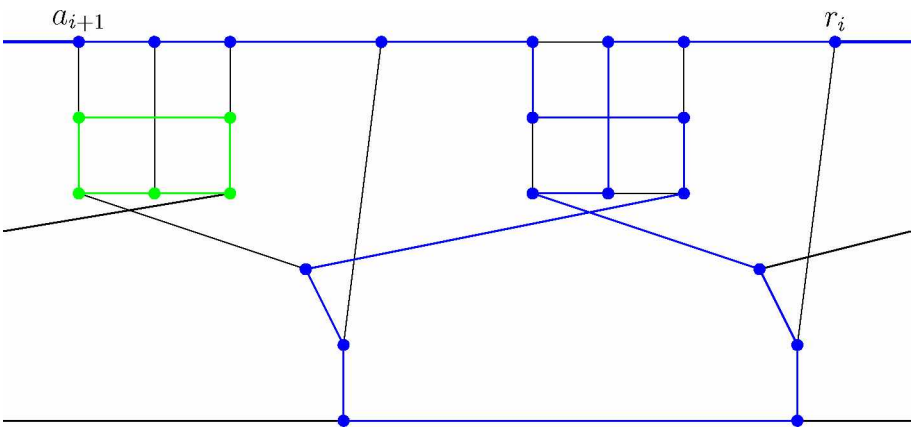

Figure 4.16: A 6-pole containing two copies of K, with a blue path on 19 vertices from r_i to a_{i+1} and a green cycle on 5 vertices that together cover the vertices of the 6-pole.

Next, if m is odd, then $\lceil \frac{m}{2} \rceil = \frac{m+1}{2}$. So, if $m \equiv 3 \mod 4$, then $m+1 \equiv 0 \mod 4$, and $\omega(\mathcal{F}_m) \geq \frac{m+1}{2}$, by applying the paragraph above. On the other hand, if $m \equiv 1 \mod 4$, then $m+1 \equiv 2 \mod 4$, so $\omega(\mathcal{F}_m) \geq \frac{m+1}{2} + 1$.

We claim that these lower bounds are in fact achieved by the graphs $\mathcal{F}_m$.

Theorem 4. *The oddness of $\mathcal{F}_m$ is*

(1.) $\omega(\mathcal{F}_m) = \frac{m}{2}$ *if* $m \equiv 0 \mod 4$,

(2.) $\omega(\mathcal{F}_m) = \frac{m+1}{2} + 1$ *if* $m \equiv 1 \mod 4$,

(3.) $\omega(\mathcal{F}_m) = \frac{m}{2} + 1$ *if* $m \equiv 2 \mod 4$,

(4.) $\omega(\mathcal{F}_m) = \frac{m+1}{2}$ *if* $m \equiv 3 \mod 4$.

Proof. We have already established that these values are lower bounds for $\omega(\mathcal{F}_m)$. To establish an upper bound, we will construct 2-factors with the given number of odd cycles for each condition on m.

We begin with the construction on even m. Starting at r_0, we draw the blue path from Figure 4.16 on $\mathcal{F}_m$, ending at a_1. We extend this path to r_2, then again follow the blue path from Figure 4.16, ending at a_3. We continue to extend the path this way, with a copy

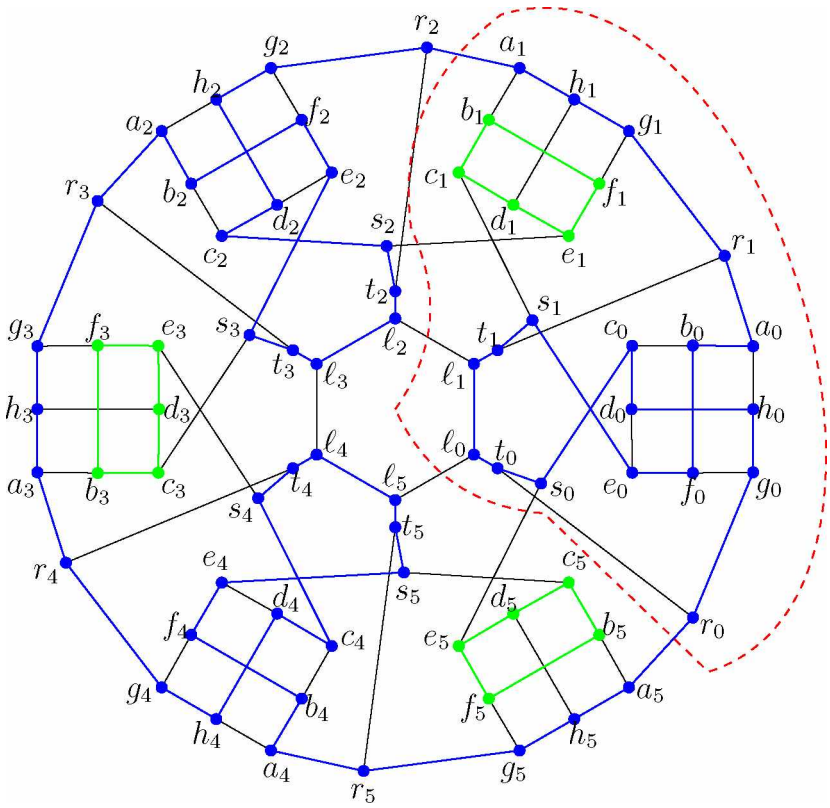

Figure 4.17: The graph $\mathcal{F}_6$ with a 2-factor composed of three 5-cycles (marked in green) and a single 57-cycle (marked in blue). As $m = 6 \equiv 2 \mod 4$, this 2-factor combined with the lower bounds from the text show that $\omega(\mathcal{F}_6) = 4$. A single copy of the subgraph from 4.16 is outlined in red.

of the path starting at $r_0, r_2, r_4, \ldots, r_{m-2}$, until we eventually return to r_0, forming a cycle. Between the large blue cycle and the smaller green cycles (which we add to cover the vertices missed by the blue cycle, as shown in Figure 4.16), every vertex in $\mathcal{F}_m$ is covered exactly once, so we have constructed a 2-factor for $\mathcal{F}_m$.

The blue path in Figure 4.16 covers 19 vertices of the subgraph, so in the final construction, the large blue cycle will have length

$$\left(\frac{m}{2}\right) 19,$$

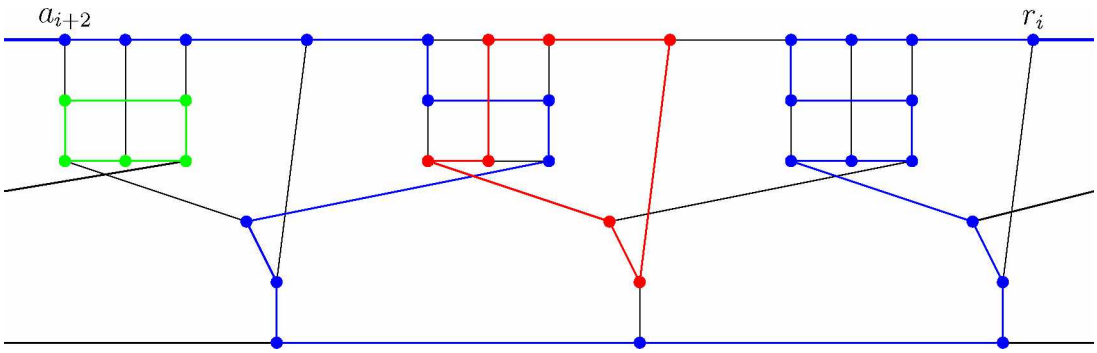

Figure 4.18: A 6-pole containing three copies of K with a blue path on 24 vertices from r_i to a_{i+2}, a green 5-cycle, and a red 7-cycle.

which is even if and only if $\frac{m}{2}$ is even. Moreover, for each copy of the subgraph in 4.16, we have a single 5-cycle, which is odd. Thus, when $m \equiv 0 \mod 4$, $\frac{m}{2}$ is even, and we have a 2-factor with $\frac{m}{2}$ odd cycles. When $m \equiv 2 \mod 4$, $\frac{m}{2}$ is odd, so we have a 2-factor with $\frac{m}{2}+1$ odd cycles. A concrete example in the case where $m = 6$ is given in Figure 4.17. The oddness in this case is 4, because $m \equiv 2 \mod 4$ and $\frac{m}{2}+1 = 4$.

Now, we will consider $\mathcal{F}_m$ when m is odd. As before, we start at r_0 and follow the blue path from Figure 4.16 to a_1, extend to r_2 and continue as before with paths starting at $r_0, r_2, r_4, \ldots$ until we reach the vertex r_{m-3}, which we must, because m is odd. At that point, we follow the blue path from Figure 4.18 from r_{m-3} to a_{m-1}, from which we can extend our path back to r_0, completing the blue cycle. We add the green 5-cycles as needed, and the single red 7-cycle indicated by Figure 4.18.

In Figure 4.18, the blue path passes through 24 vertices. Therefore, in the final graph, the blue cycle has length

$$24 + \left(\frac{m-3}{2}\right) 19,$$

which is even if and only if $\frac{m-3}{2}$ is even. This corresponds to $m \equiv 3 \mod 4$. So, this construction gives a 2-factor with

$$2 + \frac{m-3}{2} = \frac{m+1}{2}$$

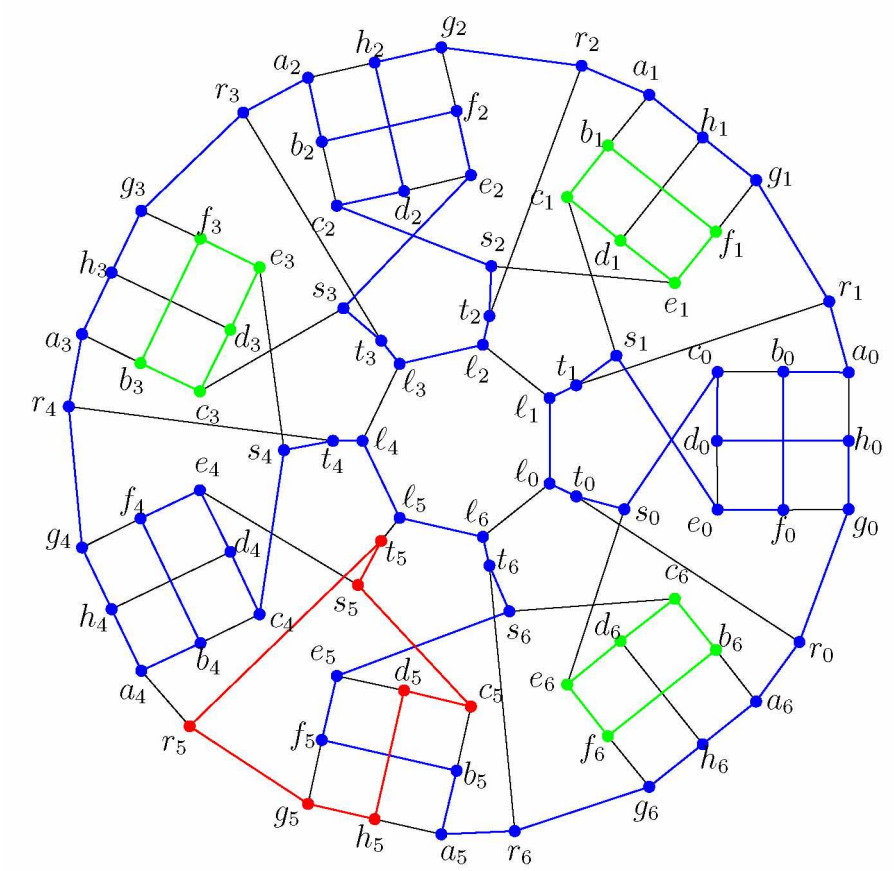

Figure 4.19: The graph $\mathcal{F}_7$, with a 2-factor containing three 5-cycles (marked in green) a single 7-cycle (marked in red), and a single 62-cycle (marked in blue), for a total of four odd cycles. As $m = 7 \equiv 3 \mod 4$, exhibiting this 2-factor combined with the lower bounds from the text shows that $\omega(\mathcal{F}_7) = 4$.

odd cycles if $m \equiv 3 \mod 4$, and

$$2 + \frac{m-3}{2} + 1 = \frac{m+1}{2} + 1$$

odd cycles if $m \equiv 1 \mod 4$. An example of a 2-factor constructed this way on $\mathcal{F}_7$ is shown in Figure 4.19.

This construction exhibits 2-factors with numbers of odd cycles achieving the lower bounds for each case of $m \mod 4$, which establishes the theorem. □

We have an equivalent result for the graphs $\mathcal{R}_m$, although as m is always even in this family, we have only two cases.

Theorem 5. *The oddness of* $\mathcal{R}_m$ *is*

(1.) $\omega(\mathcal{R}_m) = \frac{m}{2}$ *if* $m \equiv 0 \mod 4$,

(2.) $\omega(\mathcal{R}_m) = \frac{m}{2} + 1$ *if* $m \equiv 2 \mod 4$.

Proof. The lower bounds on oddness that we established previously apply equally well to the graphs $\mathcal{R}_m$, so once again, we must exhibit a construction for a 2-factor with a number of odd cycles achieving that lower bound for each of our two cases.

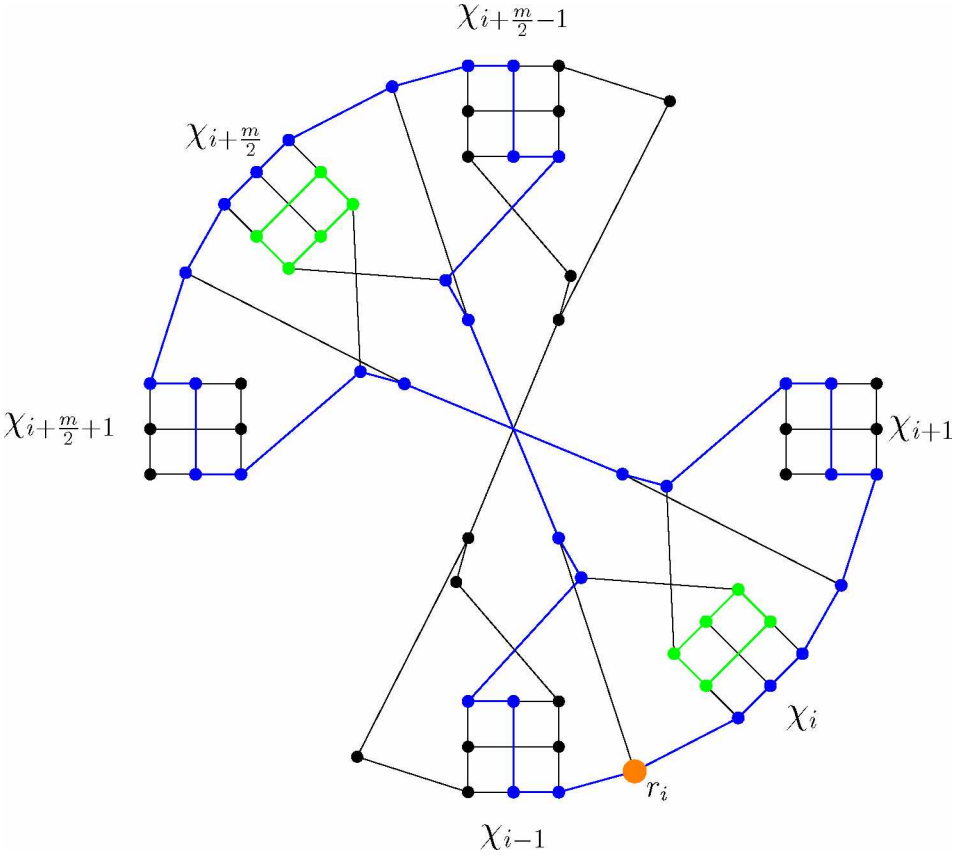

Figure 4.20: A subgraph of $\mathcal{R}_m$ with a blue 34-cycle and two green 5-cycles. Note that all the vertices in the subgraphs χ_i and $\chi_{i+\frac{m}{2}}$ are covered by these cycles. On the other hand, only some of the vertices in $\chi_{i-1}, \chi_{i+1}, \chi_{i+\frac{m}{2}-1}$ and $\chi_{i+\frac{m}{2}+1}$ are covered. The highlighted orange point r_i will be used to identify where on the graph this subgraph is located.

We will be adding copies of the cycles from Figures 4.20 and 4.23, and keeping track of where each copy the cycles is located in the graph is a nontrivial issue. To that end, we have

identified a particular vertex r_i in each of the figures, and will refer to where in the graph that vertex appears to identify the copy of the cycles.

In general terms, the strategy to create the 2-factor is to stack copies of the cycles from Figure 4.20 at two "clicks" from each other—i.e., where $r_i = r_0, r_2, r_4, \ldots$ up to $r_{m/2-2}$ if $m \equiv 0 \mod 4$. If $m \equiv 2 \mod 4$, then we begin with a copy of the subgraph from Figure 4.23 at $r_i = 0$, then continue with copies of the cycles from Figure 4.20 at $r_i = r_3, r_5, \ldots$ until we once again reach $r_{m/2-2}$.

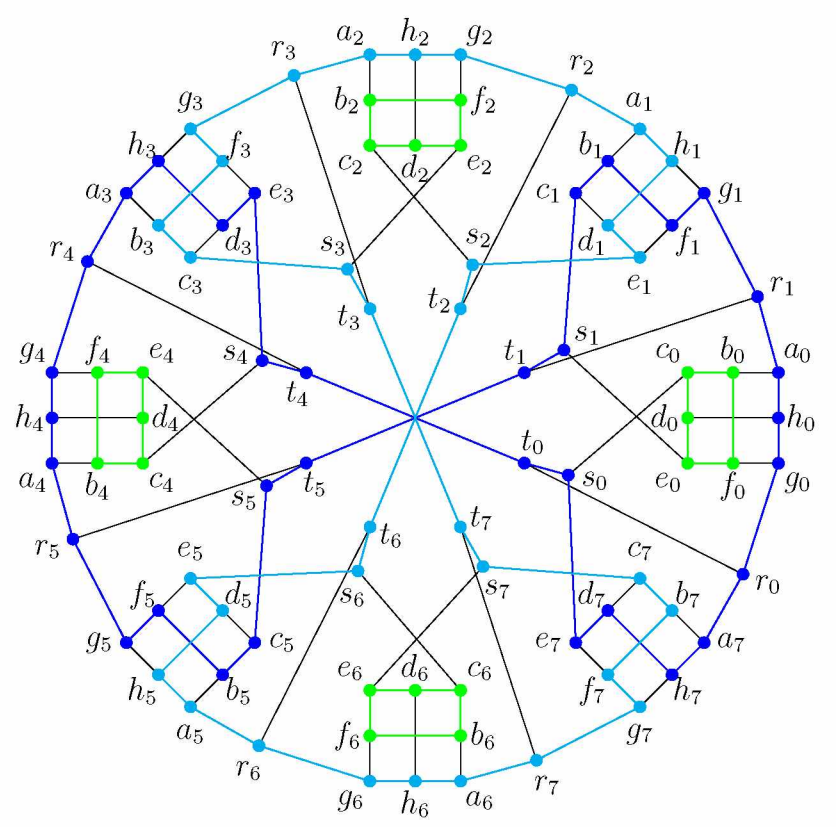

Figure 4.21: The graph $\mathcal{R}_8$ on 88 vertices. A 2-factor composed of a two copies of the 34-cycle from Figure 4.20 and four green 5-cycles is shown, which (when paired with the lower bound from the text) demonstrates that the oddness of $\mathcal{R}_8$ is 4.

More formally, we begin our construction of a 2-factor for $\mathcal{R}_m$ by inserting the cycles from Figure 4.20 with $r_i = r_0$. Notice that the blue and green cycles in Figure 4.20 cover the vertices of the subgraphs χ_0 and $\chi_{\frac{m}{2}}$. To cover the remaining vertices in χ_1 and $\chi_{\frac{m}{2}+1}$, we add another copy of the cycles from Figure 4.20 identified by $r_i = r_2$. The blue cycles

interlace and, when $m \equiv 0 \mod 4$, we can repeat this process with copies of the cycles with $r_i = r_4, r_6, \ldots$ until we eventually add cycles corresponding to $r_{m/2-2}$, which interlace to cover the remaining vertices in χ_{m-1} and $\chi_{\frac{m}{2}-1}$, completing the 2-factor.

This discussion has focused on the vertices in the subgraphs χ_i, but by the design of the cycles in Figure 4.20, the remaining vertices are covered as well. An example of this process is shown in Figure 4.21 on $\mathcal{R}_8$. Following this technique, we construct a 2-factor with $\frac{m}{4} \cdot 2 = \frac{m}{2}$ odd cycles, which achieves the lower bound for the case when $m \equiv 0 \mod 4$.

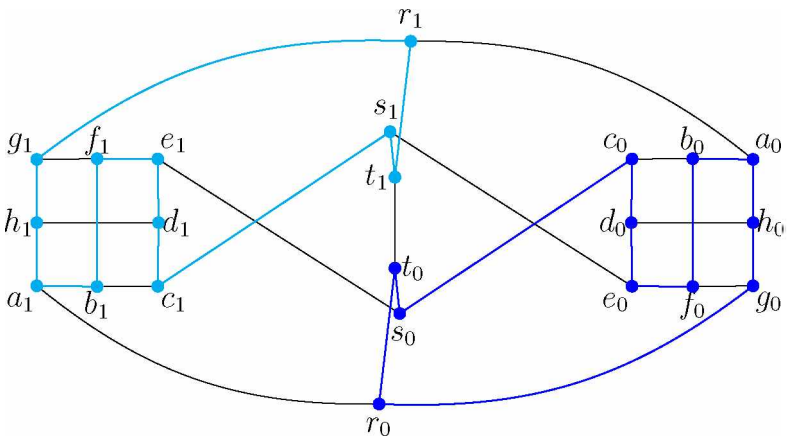

Figure 4.22: The graph $\mathcal{R}_2$ with two 11-cycles shown in blue and cyan, demonstrating that the oddness is 2.

When $m \equiv 2 \mod 4$, we have two cases. When $m = 2$, we can compute the oddness directly: as $\mathcal{R}_2$ is a snark, we know the oddness is not 0, and Figure 4.22 demonstrates a 2-factor with two 11-cycles. This shows that the oddness is 2, which is consistent with the theorem.

For $m \geq 6$, we construct our 2-factor in a similar fashion to the technique we used for $m \equiv 0 \mod 4$. However, instead of beginning by inserting a copy of the cycles in Figure 4.20 with $r_i = r_0$, we insert a copy of the cycles in Figure 4.23 for $r_i = r_0$. We then proceed as before, adding copies of the cycles from Figure 4.20 at $r_i = r_3, r_5, \ldots$ until we reach $r_{m/2-2}$, which we know we will because when $m \equiv 2 \mod 4$, we know that $m/2$ will be odd. As before, when we add the $r_{m/2-2}$ copy, the cycles interlace with the r_0 cycles and complete the

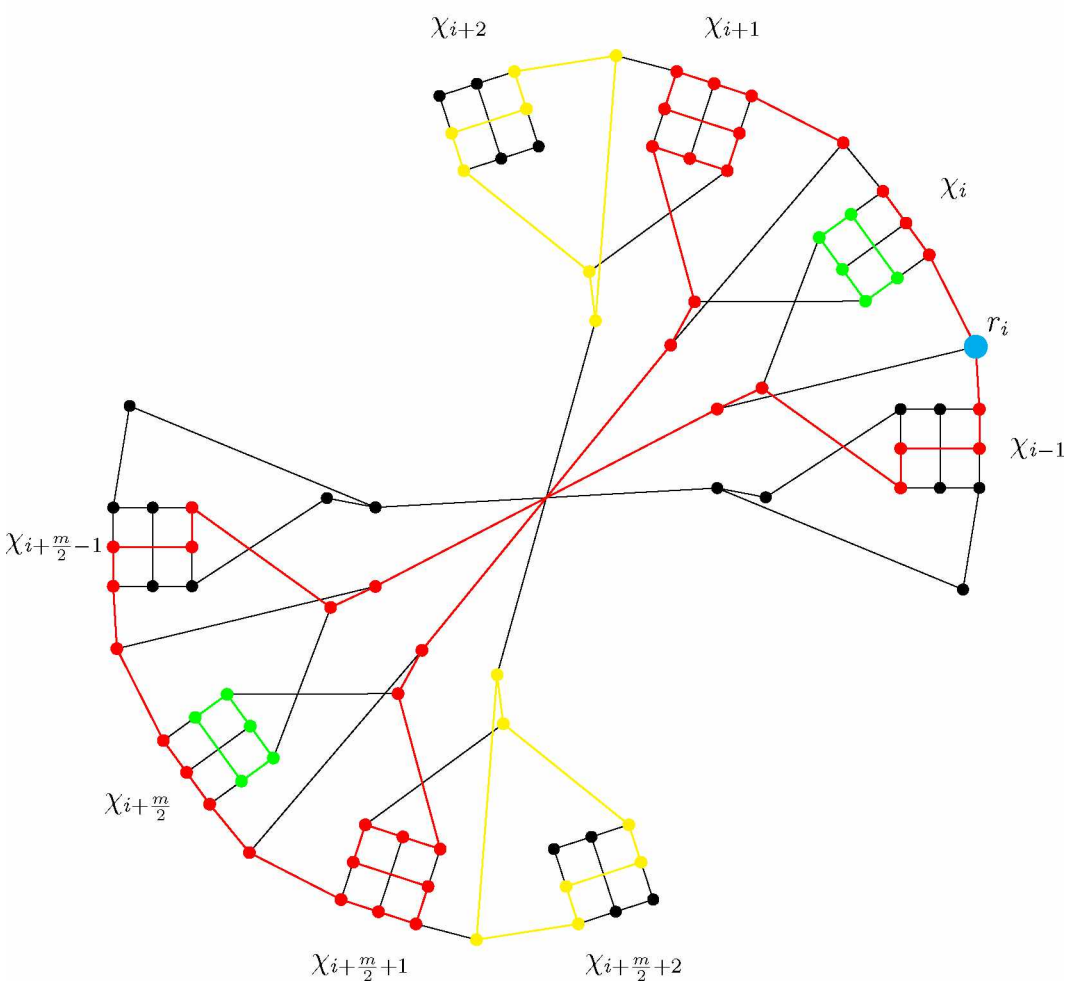

Figure 4.23: A subgraph of $\mathcal{R}_m$ with a red 42-cycle, two yellow 7-cycles, and two green 5-cycles. Note that the red 42-cycle is very similar to the blue 34-cycle in Figure 4.20, but it covers all the vertices of χ_{i+1} and $\chi_{i+\frac{m}{2}+1}$. The large cyan point r_i will be used to identify where in the graph these cycles will be added.

2-factor. An example of this process is shown in Figure 4.24. This gives a 2-factor composed of:

- the two yellow 7-cycles from Figure 4.23;
- two green 5-cycles from Figure 4.23;
- $\frac{m-6}{4} \cdot 2 = \frac{m-6}{2}$ green 5-cycles from the copies of the 8-pole in Figure 4.20;
- a single 42-cycle from Figure 4.23;
- $\frac{m-6}{4}$ 34-cycles from Figure 4.20.

This gives us a 2-factor with

$$4 + \frac{m-6}{2} = \frac{m}{2} + 1$$

odd cycles. As this achieves the lower bound for the case when $m \equiv 2 \mod 4$, this completes the proof of the theorem. □

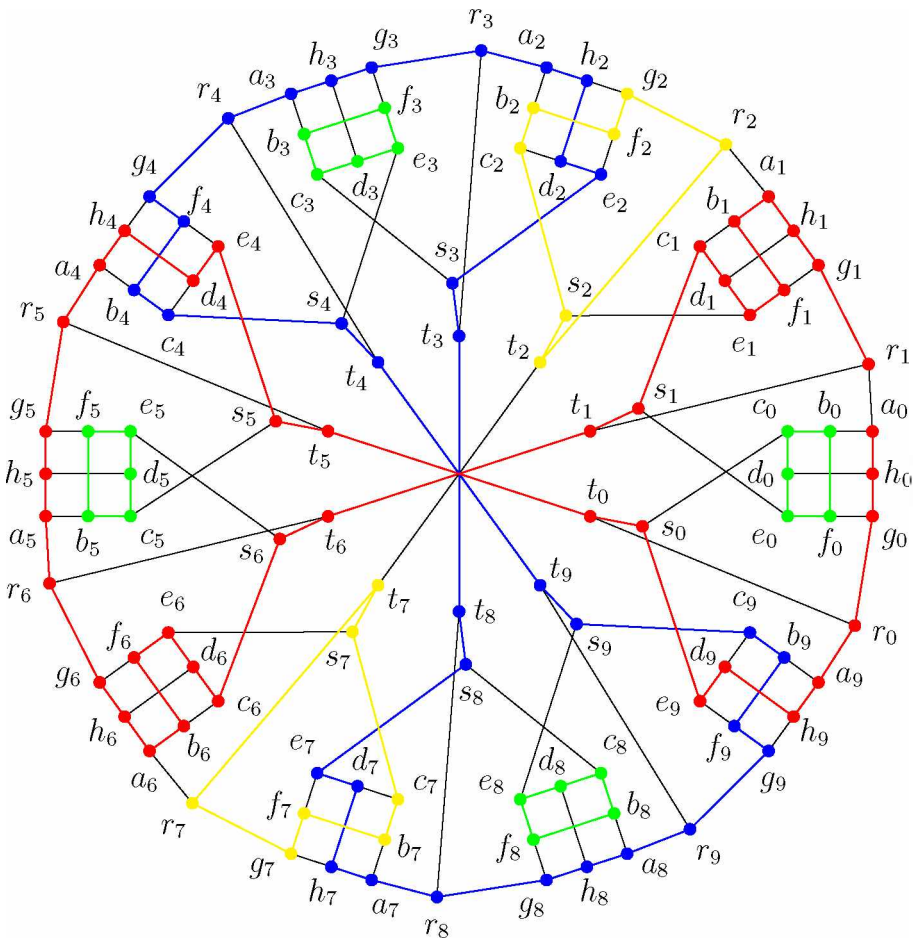

Figure 4.24: The graph $\mathcal{R}_{10}$ on 110 vertices, with a blue cycle on 34 vertices, a red cycle on 42 vertices, four green 5-cycles, and two yellow 7-cycles, demonstrating the oddness of $\mathcal{R}_{10}$ is 6, when paired with the lower bound from the text.

Chapter 5: Conclusions and Open Questions

In this paper, we outlined the construction of two infinite families of snarks, the graphs $\mathcal{F}_m$ and $\mathcal{R}_m$. In showing that these graphs are indeed snarks, we uncovered an unusual "oriented" coloring property of the 5-pole K that forced any 3-edge-coloring to have matching semiedges on the "left" side, and mismatching on the "right," a property that as far as we know, has not been used to construct snarks before. This leads to the first open question: are there other graphs that when converted to 5-poles, have this property? If so, the construction here presented should carry through immediately to find new families of snarks.

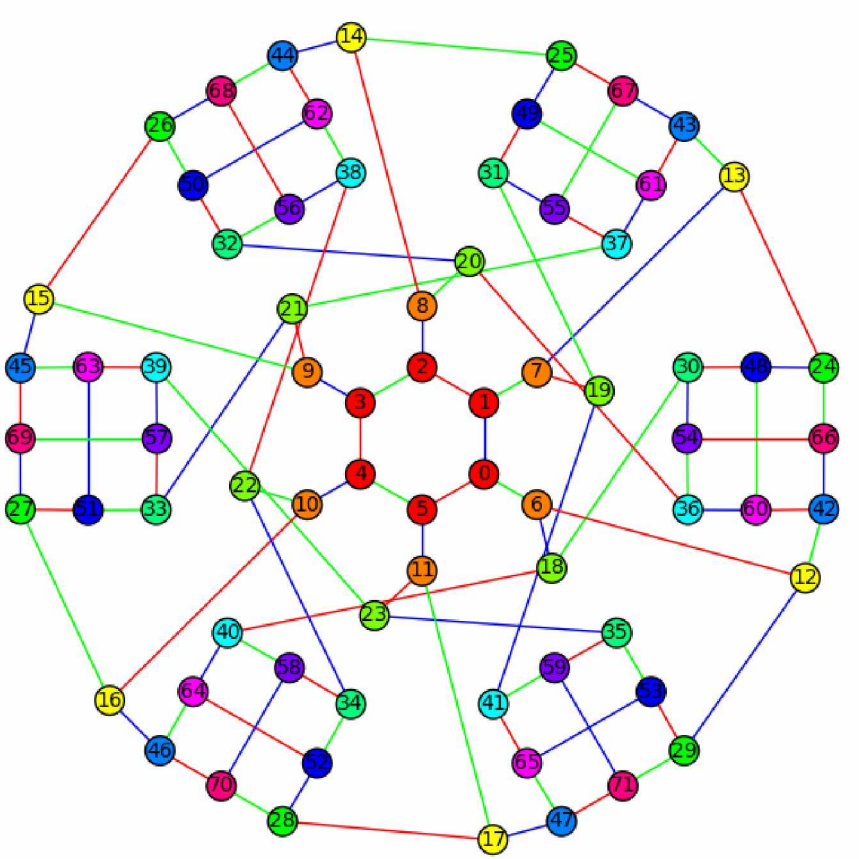

Figure 5.1: The graph $G(6, 1, 2, 1)$ with a 3-edge-coloring, produced by the mathematical analysis software Sage [16].

Of note, while we focused on the graphs $\mathcal{F}_m$ and $\mathcal{R}_m$, we showed that $G_v(m, \alpha, \alpha, 1)$ and $G_{dv}(m, \alpha, \alpha)$ are snarks. However, it is not settled whether $G_v(m, \alpha, \beta, \gamma)$ is 3-edge-colorable

for any $\alpha \neq \beta$. For small cases, it is certainly true that these graphs are 3-edge-colorable (an example of a 3-edge-coloring for $G(6,1,2,1)$ is presented in Figure 5.1), but it is not known whether for large m, some divisibility constraint prevents a valid 3-edge-coloring.

Conjecture 1. *The graphs $G_v(m,\alpha,\beta,\gamma)$ are 3-edge-colorable for $\alpha \neq \beta$.*

We explored the connection between the families $\mathcal{F}_m$ and $\mathcal{R}_m$ and the blowup construction presented by Hägglund in [8], as well as the automorphism groups of $\mathcal{F}_m$ and $\mathcal{R}_m$. We can view the automorphism group of $\mathcal{F}_m$ as being "partitioned" into a subgroup that is isomorphic to a subgroup of the automorphism group of the underlying graph that the blowup was performed on (the m-prism for $\mathcal{F}_m$) and new automorphisms that came from the blowup construction. We don't in general obtain the entire automorphism group of the underlying graph as a subgroup: the m-prism has an automorphism interchanging the inner and outer cycles that is lost when the blowup is performed only around the outer cycle. Can we make formal exactly what subgroup of the underlying graph's automorphism group is preserved, and generalize this to all blowup constructions to at least achieve a lower bound on the size of the automorphism group of the blowup?

References

[1] K. Appel and W. Haken, *Every planar map is four colorable*, Bulletin of the American mathematical Society, 82 (1976), pp. 711–712.

[2] L. W. Berman, D. Oliveros, and G. I. Williams, *Cyclic pseudo-Loupekine snarks*. preprint, University of Alaska Fairbanks, Fairbanks, 2019.

[3] G. Brinkmann, K. Coolsaet, J. Goedgebeur, and H. Mélot, *House of graphs: A database of interesting graphs*, Discrete Applied Mathematics, 161 (2013), pp. 311–314, https://doi.org/10.1016/j.dam.2012.07.018.

[4] B. Descartes, *Network-colourings*, The Mathematical Gazette, 32 (1948), p. 67, https://doi.org/10.2307/3610702.

[5] M. Gardner, *Mathematical games: Snarks, boojums and other conjectures related to the four-color-map theorem*, Scientific American, 234 (1976), pp. 126–131.

[6] J. L. Gross and T. W. Tucker, *Topological Graph Theory*, Dover Publications Inc., 2003, https://www.ebook.de/de/product/3355571/jonathan_l_gross_thomas_w_tucker_topological_graph_theory.html.

[7] R. Häggkvist and S. McGuinness, *Double covers of cubic graphs with oddness 4*, Journal of Combinatorial Theory, Series B, 93 (2005), pp. 251–277, https://doi.org/10.1016/j.jctb.2004.11.003.

[8] J. Hägglund, *On snarks that are far from being 3-edge colorable*, Electronic Journal of Combinatorics, 23 (2016), pp. Paper 2.6, 10.

[9] A. Huck and M. Kochol, *Five cycle double covers of some cubic graphs*, Journal of Combinatorial Theory, Series B, 64 (1995), pp. 119–125, https://doi.org/10.1006/jctb.1995.1029.

[10] R. Isaacs, *Infinite families of nontrivial trivalent graphs which are not Tait colorable*, The American Mathematical Monthly, 82 (1975), pp. 221–239.

[11] R. Isaacs, *Loupekine's snarks: A bifamily of non-tait-colorable graphs*, Tech. Report 263, The Johns Hopkins University, Nov. 1976.

[12] F. Jaeger, *A survey of the cycle double cover conjecture*, in North-Holland Mathematics Studies, vol. 115, Elsevier, 1985, pp. 1–12.

[13] R. Lukot'ka, E. Máčajová, J. Mazák, and M. Škoviera, *Small snarks with large oddness*, Electronic Journal of Combinatorics, 22 (2015), pp. Paper 1.51, 20.

[14] R. Nedela and M. Škoviera, *Decompositions and reductions of snarks*, Journal of Graph Theory, 22 (1996), pp. 253–279, https://doi.org/10.1002/(sici)1097-0118(199607)22:3<253::aid-jgt6>3.0.co;2-l.

[15] P. D. Seymour, *On multicolourings of cubic graphs, and conjectures of Fulkerson and Tutte*, Proceedings of the London Mathematical Society. Third Series, 38 (1979), pp. 423–460, https://doi.org/10.1112/plms/s3-38.3.423.

[16] The Sage Developers, *SageMath, the Sage Mathematics Software System (Version 8.5)*, 2018. https://www.sagemath.org.

[17] J. J. Watkins, *Snarks*, Annals of the New York Academy of Sciences, 576 (1989), pp. 606–622.

[18] D. B. West, *Introduction to Graph Theory (2nd Edition)*, Pearson, 2000.